T.R.
SAKARYA UNIVERSITY
GRADUATE SCHOOL OF NATURAL AND APPLIED SCIENCES

INVESTIGATION OF THE PARAMETERS AFFECTING SHEAR CAPACITY OF RC BEAMS USING NUMERICAL SIMULATIONS

MSc THESIS

Fazıl Abdulkadir ÇAĞLAR

Deparment of Civil Engineering

Structure Programme

DECEMBER 2023

T.R.
SAKARYA UNIVERSITY
GRADUATE SCHOOL OF NATURAL AND APPLIED SCIENCES

INVESTIGATION OF THE PARAMETERS AFFECTING SHEAR CAPACITY OF RC BEAMS USING NUMERICAL SIMULATIONS

MSc THESIS

Fazıl Abdulkadir ÇAĞLAR

Department of Civil Engineering

Structure Programme

Thesis Advisor: Assoc. Prof. Dr. Aydın DEMİR

DECEMBER 2023

The thesis work titled “Investigation of the Parameters Affecting Shear Capacity of RC Beams using Numerical Simulations” prepared by Fazıl Abdulkadir ÇAĞLAR was accepted by the following jury on 22/12/2023 by unanimously/majority of votes as a MSc THESIS in Sakarya University Graduate School of Natural and Applied Sciences, İnşaat Mühendisliği department, Yapı programe.

Thesis Jury

Head of Jury :	**Assoc. Prof. Dr. Sedat SERT** Sakarya University	.....
Jury Member :	**Assoc. Prof. Dr. Aydın DEMİR** Sakarya University	.....
Jury Member :	**Assist. Prof. Dr. Gökhan DOK** Sakarya University of Applied Sciences	.....

STATEMENT OF COMPLIANCE WITH THE ETHICAL PRINCIPLES AND RULES

I declare that the thesis work titled " INVESTIGATION OF THE PARAMETERS AFFECTING SHEAR CAPACITY OF RC BEAMS USING NUMERICAL SIMULATIONS", which I have prepared in accordance with Sakarya University Graduate School of Natural and Applied Sciences regulations and Higher Education Institutions Scientific Research and Publication Ethics Directive, belongs to me, is an original work, I have acted in accordance with the regulations and directives mentioned above at all stages of my study, I did not get the innovations and results contained in the thesis from anywhere else, I duly cited the references for the works I used in my thesis, I did not submit this thesis to another scientific committee for academic purposes and to obtain a title, in accordance with the articles 9/2 and 22/2 of the Sakarya University Graduate Education and Training Regulation published in the Official Gazette dated 20.04.2016, a report was received in accordance with the criteria determined by the graduate school using the plagiarism software program to which Sakarya University is a subscriber, I accept all kinds of legal responsibility that may arise in case of a situation contrary to this statement.

(…/12/2023)

Fazıl Abdulkadir ÇAĞLAR

ACKNOWLEDGMENTS

I would like to thank my esteemed advisor Mr. Aydın DEMİR, from whom I benefited from his knowledge and experience throughout my master's degree education, for his help in all stages of the research from planning to writing.

I owe a debt of gratitude to my very valuable Mrs. Tuba TATAR, who has always supported me in this long process, created new horizons with the answers to my questions, and I am pleased to work and learn with her. I would like to thank Mr. Erkan BİÇİCİ and Mr. Ali SARIBIYIK for their remarkable contribution to the numerical section.

I would like to express my endless gratitude and thanks to my esteemed father Naci, my mother Berna and my siblings Edibe Beyza, Ahmet Necib and Mehmet Muhsin, each of whom I love very much, who have provided me with all kinds of material and moral support throughout my life, guided me in every subject, and helped me come to this day without sparing their sacrifices.

I would like to thank my beloved wife Şadiye Nur for her patience, understanding and support throughout my master's degree education and my daughter Edibe Meryem, who was born during my education and who gave me strength, happiness and joy with her presence.

Fazıl Abdulkadir ÇAĞLAR

TABLE OF CONTENTS

Page

ABBREVIATIONS

a : Equivalent rectangular compression block depth, k_1c

a/d : Shear span to depth ratio

b_w : Smallest width of the cross-section in the tensile area (mm)

CDP : Concrete Damage Plastisity

C : Concrete

d : Effective depth in case of flexural members

d_c : Damage parameter of concrete at axial compression condition

d_t : Damage parameter of concrete at axial tension condition

E : Young module

f_{ck} : Characteristic concrete compressive strength

f_{ct} : Maximum tensile stress of concrete

f_{ywd} Transverse reinforcement design yielding stress.

h : Overall depth of specimen

FE : Finite elements

P_u : Maximum load carrying capacity

u_u : Maximum displacement

V_c : Concrete contribution to shear strength

V_{cr} : Crack resistance of the section in shear

V_d : Design shear force

V_r : Shear strength

V_w : Contribution of shear reinforcement to shear strength

$V_{Rd,c}$: Design shear resistance of the member without shear reinforcement

$V_{Rd,s}$: Design value of the shear force which can be sustained by the yielding shear reinforcement

$V_{Rd,max}$: Design value of the maximym shear force which can be sustained by the member, limited by crushing of the compression struts.

V_{ccd} : Design value of the shear component of the force in the compression area, in case of an inclined compression chord

V_{td} : Design value of the shear component of the force in the tensile reinforcement, in the case of an inclined tensile chord

SYMBOLS

ε	: Strain
ε_c	: Strain of concrete
ε_{cr}	: Cracking strain
ε_c^{in}	: Elastic strain of concrete
ε_t	: Tensile strain of concrete
σ	: Stress
σ_c	: Stress of concrete
σ_t	: Tensile stress of concrete

LIST OF TABLES

Page

LIST OF FIGURES

Page

INVESTIGATION OF THE PARAMETERS AFFECTING SHEAR CAPACITY OF RC BEAMS USING NUMERICAL SIMULATIONS

SUMMARY

The mechanism of shear damage and crack control in reinforced concrete beams has been studied and analysed by many researchers for a long time. Considering rapid development of computer technology and the resulting computational programs, the behavior of beams, columns and structures can be simulated. However, it is still contraveial exactly how accurate these models can reflect the behavior of structures,elements and/or sections. In this study, the parameters affecting the shear capacity of reinforced concrete beams in numerical modelling employing a commertial program are investigated and the capacity and limitations of numerical modelling under the title of shear damage mechanism are criticised.

In reinforced concrete frame structures, beams are most commonly used as part of the load-bearing system in almost all countries. In many countries, including Turkey, reinforced concrete is a widely used structural material in civil engineering. The main reasons for the widespread use of reinforced concrete are that the materials that make up the concrete and the reinforcement are easy to find and cheaper than other construction techniques.

The reinforced concrete used in buildings has two main functions: To transfer horizontal and vertical loads. Its first task is to transfer the horizontal loads acting on the support system, particularly those due to wind and seismic loads, to the vertical support elements together with the floors. The second is to transfer the dead and live loads transferred from the floor and the wall loads, if any, with columns or shears. In addition, through this transfer, the vertical members share the loads in proportion to their stiffness. Under this heading, reinforced concrete beams are mentioned.

In cross sections, axial force and bending moment create normal stress, while shear force and torsion moment create shear stress. Depending on the loading in the beams, the value of the shear force changes along the beam length. The fracture form of a beam, which is also under the influence of shear force, is quite complex; It varies depending on the loading, the distance of the load from the support, the depth of the beam, the concrete compressive strength, and the amount and arrangement of the tension and shear reinforcements. The cracks occurring in the selected continuous beam as an example are given schematically.

Shear cracking in reinforced concrete elements and control of this cracking has been tried to be calculated for decades. The correct calculation and prevention of this damage is very important. Because, as civil engineers, our expectation from reinforced concrete elements is that the type of damage is realised at once, giving people the time to escape in disasters such as earthquakes.

In this study, a shear damage collapse experiment was selected from the literature. Reinforced concrete beams were modelled using the finite element method and the behaviour of the beams was investigated using a numerical model. The analyses were

carried out using the ABAQUS finite element method with the concrete damage plasticity (BHP) model for concrete and the classical metal plasticity model for reinforcing steel. The compressive and tensile values for concrete, yield strength and ultimate tensile strength for reinforcement were used in the experiment selected from the literature to create the material model. The results obtained from the numerical models show that the concrete damage plasticity model can accurately represent the behaviour of reinforced concrete beams with shear collapse damage under static loading.

Within the scope of this thesis study, 2 tested beams are considered. Similar size beams were designed with the specimens used in the experimental study. First, modeling was done for the beam in which the stirrups were installed at 80 mm intervals. Keeping the stirrup yield strength constant, 6 beam models were made for different stirrup thicknesses.

In this way, a total of 36 beams were modeled for different stirrup yield strengths. 18 of these models are for 80 mm stirrup spacing and 18 for 120 mm stirrup spacing.

A parametric study was carried out for two different stirrup spacings using two of the validated numerical models. In the parametric studies, the stirrup spacing, material properties and size were kept constant. As the stirrup thickness was increased, the change in the shear load of the reinforced concrete beams was observed. Subsequently, parametric studies were carried out for S220 steel and S420 steel, keeping the stirrup thickness constant.

The second chapter consists of 5 sub-headings. In the first subheading, general information about the behaviour of reinforced concrete beams is given. In the second subheading, types of collapse of reinforced concrete beams are given. In the third subheading, shear damage calculation formulae in American, European and Turkish standards are given. In the fourth subheading, studies in the literature on shear damage mechanism are given. In the last subheading, a general information about finite element modelling is given.

There are 5 sub-headings in the third chapter. The first subheading is Methodology. In this chapter, assumptions, finite element method and details are explained. In the second subheading, the experiments performed in the literature and used in this thesis and their results are explained in detail. The third subheading describes the modelling of the experiment in ABAQUS and the verification of the results. The fourth subsection describes the calibration process of the modelling and the parameters to be considered for future numerical studies. In the fifth and final section, a parametric study is carried out by increasing the thickness of the validated model stirrups and increasing the tensile strength of the stirrups.

The results of the numerical and parametric study are given in the fourth section.

The results of the parametric study for ST80 beam with stirrup yield strength fy = 310 MPa. In the graph, it is seen that as the stirrup thickness increases, the midpoint maximum displacement value and the maximum shear loads taken by the specimens before failure increase. The midpoint displacement value of the ST80_55_310 model is 7.09 mm. The maximum shear load of the specimen at this displacement value is 124.68 kN. The midpoint displacement value of ST80_100_310 model is 7.95 mm. The maximum shear load of the specimen at this displacement value is 135.39 kN.

It is seen that shear failure in reinforced concrete beams can be modelled successfully by finite element method. However, parametric studies show that as the stirrup

thickness in the numerical models is increased, the shear force that the reinforced concrete beams can withstand does not increase as much as it increases in the regulations.

Numerical modelling of shear failure of reinforced concrete beams, beam-truss difference is presented. Beam models were found to reflect the shear failure behaviour much better than truss models.

BETONARME KİRİŞLERDE KESME KAPASİTESİNİ ETKİLEYEN PARAMETRELERİN SAYISAL MODELLEME YÖNTEMLERİNDE İRDELENMESİ

ÖZET

Betonarme kirişlerde kesme hasarı mekanizması ve çatlak kontrolü birçok araştırmacı tarafından uzun süredir incelenmekte ve analiz edilmektedir. Bilgisayar teknolojisinin gelişmesi ve ortaya çıkan programlar sayesinde kirişler, kolonlar ve yapılar modellenebilmektedir. Ancak bu modellerin deneyleri, kodları ve gerçeği ne kadar iyi yansıttığı tam olarak bilinmemektedir. Bu çalışmada, sayısal modelleme yöntemlerinde betonarme kirişlerin kesme kapasitesini etkileyen parametreler incelenmiş ve kesme hasar mekanizması başlığı altında sayısal modellemenin yeterliliği ve sınırlamaları eleştirilmiştir.

Betonarme çerçeve yapılarda kirişler, hemen hemen tüm ülkelerde taşıyıcı sistemin bir parçası olarak en yaygın şekilde kullanılmaktadır. Türkiye de dahil olmak üzere birçok ülkede betonarme, inşaat mühendisliğinde yaygın olarak kullanılan bir yapı malzemesidir. Betonarmenin yaygın olarak kullanılmasının başlıca nedenleri, betonu ve donatıyı oluşturan malzemelerin kolay bulunması ve diğer yapım tekniklerine göre daha ucuz olmasıdır.

Binalarda kullanılan betonarmenin iki ana işlevi vardır: Yatay ve düşey yükleri aktarmak. Birinci görevi, taşıyıcı sisteme etkiyen yatay yükleri, özellikle rüzgâr ve deprem yüklerinden kaynaklananları, döşemelerle birlikte düşey taşıyıcı elemanlara aktarmaktır. İkincisi ise döşemeden aktarılan ölü ve hareketli yükleri ve varsa duvar yüklerini kolon veya makaslarla aktarmaktır. Ayrıca bu aktarım sayesinde düşey elemanlar rijitlikleri oranında yükleri paylaşırlar. Bu başlık altında betonarme kirişlerden bahsedilmektedir.

Kesitlerde eksenel kuvvet ve eğilme momenti normal gerilme oluştururken, kesme kuvveti ve burulma momenti kayma gerilmesi oluşturur. Kirişlerdeki yüklemeye bağlı olarak kesme kuvvetinin değeri kiriş uzunluğu boyunca değişmektedir. Kesme kuvveti etkisinde de olan bir kirişin kırılma şekli oldukça karmaşıktır; yüklemeye, yükün mesnetten uzaklığına, kirişin derinliğine, beton basınç dayanımına, çekme ve kesme donatılarının miktarına ve düzenine bağlı olarak değişir. Örnek olarak seçilen sürekli kirişte meydana gelen çatlaklar şematik olarak verilmiştir.

Betonarme elemanlarda kesme çatlaması ve bu çatlamanın kontrolü onlarca yıldır hesaplanmaya çalışılmaktadır. Bu hasarın doğru hesaplanması ve önlenmesi çok önemlidir. Çünkü inşaat mühendisleri olarak betonarme elemanlardan beklentimiz, hasar türünün bir anda gerçekleşmesi, deprem gibi afetlerde insanlara kaçacak zaman tanınmasıdır.

Bu çalışmada, literatürden bir kesme hasarlı göçme deneyi seçilmiştir. Betonarme kirişler sonlu elemanlar yöntemi kullanılarak modellenmiş ve kirişlerin davranışı sayısal bir model kullanılarak incelenmiştir. Analizler ABAQUS sonlu elemanlar

yöntemi kullanılarak beton için beton hasar plastisite (BHP) modeli ve donatı çeliği için klasik metal plastisite modeli ile gerçekleştirilmiştir. Malzeme modelini oluşturmak için literatürden seçilen deneyde beton için basınç ve çekme değerleri, donatı için akma dayanımı ve nihai çekme dayanımı kullanılmıştır. Sayısal modellerden elde edilen sonuçlar, beton hasar plastisite modelinin statik yükleme altında kesme göçmesi hasarlı betonarme kirişlerin davranışını doğru bir şekilde temsil edebildiğini göstermektedir.

Bu tez çalışması kapsamında test edilen 2 kiriş ele alınmıştır. Deneysel çalışmada kullanılan numuneler ile benzer boyutta kirişler tasarlanmıştır. İlk olarak etriyelerin 80 mm aralıklarla yerleştirildiği kiriş için modelleme yapılmıştır. Etriye akma dayanımı sabit tutularak farklı etriye kalınlıkları için 6 adet kiriş modeli yapılmıştır.

Bu şekilde farklı etriye akma dayanımları için toplam 36 kiriş modellenmiştir. Bu modellerin 18 tanesi 80 mm etriye aralığı için, 18 tanesi ise 120 mm etriye aralığı içindir.

Doğrulanan sayısal modellerden ikisi kullanılarak iki farklı etriye aralığı için parametrik bir çalışma gerçekleştirilmiştir. Parametrik çalışmalarda etriye aralığı, malzeme özellikleri ve boyutu sabit tutulmuştur. Etriye kalınlığı arttıkça betonarme kirişlerin kesme yükündeki değişim gözlemlenmiştir. Daha sonra, etriye kalınlığı sabit tutularak S220 çeliği ve S420 çeliği için parametrik çalışmalar gerçekleştirilmiştir.

İkinci bölüm 5 alt başlıktan oluşmaktadır. Birinci alt başlıkta betonarme kirişlerin davranışı hakkında genel bilgiler verilmiştir. İkinci alt başlıkta betonarme kirişlerin göçme tipleri verilmiştir. Üçüncü alt başlıkta Amerikan, Avrupa ve Türk standartlarındaki kesme hasarı hesap formülleri verilmiştir. Dördüncü alt başlıkta kayma hasarı mekanizması ile ilgili literatürdeki çalışmalar verilmiştir. Son alt başlıkta ise sonlu eleman modellemesi hakkında genel bir bilgi verilmiştir.

Üçüncü bölümde 5 alt başlık bulunmaktadır. İlk alt başlık Metodoloji'dir. Bu bölümde varsayımlar, sonlu elemanlar yöntemi ve detaylar açıklanmıştır. İkinci alt başlıkta literatürde yapılan ve bu tezde kullanılan deneyler ve sonuçları detaylı olarak açıklanmıştır. Üçüncü alt başlıkta deneyin ABAQUS'ta modellenmesi ve sonuçların doğrulanması anlatılmaktadır. Dördüncü alt bölümde modellemenin kalibrasyon süreci ve gelecekteki sayısal çalışmalar için dikkate alınması gereken parametreler açıklanmaktadır. Beşinci ve son bölümde, doğrulanan model etriyelerin kalınlığı artırılarak ve etriyelerin çekme mukavemeti yükseltilerek parametrik bir çalışma gerçekleştirilmiştir.

Sayısal ve parametrik çalışmanın sonuçları dördüncü bölümde verilmiştir.

Etriye akma dayanımı fy = 310 MPa olan ST80 kirişi için yapılan parametrik çalışmanın sonuçları Şekil 4.9'da verilmiştir. Grafikte, etriye kalınlığı arttıkça orta nokta maksimum yer değiştirme değerinin ve numunelerin göçmeden önce aldığı maksimum kesme yüklerinin arttığı görülmektedir. ST80_55_310 modelinin orta nokta yer değiştirme değeri 7,09 mm'dir. Bu yer değiştirme değerinde numunenin maksimum kesme yükü 124,68 kN'dur. ST80_100_310 modelinin orta nokta yer değiştirme değeri 7,95 mm'dir. Bu yer değiştirme değerinde numunenin maksimum kesme yükü 135,39 kN'dir.

Betonarme kirişlerde kesme göçmesinin sonlu elemanlar yöntemi ile başarılı bir şekilde modellenebildiği görülmektedir. Ancak parametrik çalışmalar, sayısal modellerde etriye kalınlığı arttıkça betonarme kirişlerin dayanabileceği kesme kuvvetinin yönetmeliklerde arttığı kadar artmadığını göstermektedir.

Betonarme kirişlerin kesme göçmesinin sayısal modellemesi, kiriş-kafes farkı sunulmuştur. Kiriş modellerinin kayma göçmesi davranışını kafes modellerden çok daha iyi yansıttığı bulunmuştur.

1. INTRODUCTION

1.1. Scope of the Thesis

Indirect cracks caused by principal tensile stresses in reinforced concrete elements are dangerous because they are sudden and brittle. The domain of this study is shear failure mechanism. The shear strength of the beams was calculated by parametric study with the design codes in the literature. These calculations were compared with both the experimental results and the results of the parametric study. The capacity of numerical modelling, its pros and cons and it is aimed to be a guide for new researchers.

1.2. Purpose of Thesis

Nowadays, almost all structures are designed in a computerised environment in accordance with the regulations in the literature. In order to do this, the shear capacity in the designed structures and the results of the formulae used to calculate the shear capacity in the regulations must match. The aim of this thesis is to investigate the parameters affecting the shear capacity of shear reinforced concrete beams using numerical modelling.

1.3. Research Objectives and Layout of Work

The aim of this study is to determine how much the parameters affecting the shear capacity of reinforced concrete beams reflect the numerical models, their effects and the experiments. In addition, it is to reach a conclusion about how our colleagues working on this subject should use these parameters.

Chapter 2 gives an overview of beam behaviour and damage types. It gives formulae for shear capacity according to design codes in different regulations. Relevant studies in the literature are investigated and presented. Finally, an overview of finite element modelling is also given.

Chapter 3 describes the methodology, assumptions, the finite element method and the programme and its details. In addition, details about the experiment selected from the

literature and used in this thesis are given. Then, the developed numerical model and the calibration process while modelling this model are explained in detail. Finally, the parametric study performed from the validated model is explained.

Chapter 4, the results of the numerical modelling and parametric study are given.

Chapter 5, conclusion and future works, suggestions are given.

2. LITERATURE REVIEW

2.1. Behavior of RC Beam

In reinforced concrete frame structures, beams are most commonly used as part of the load-bearing system in almost all countries. In many countries, including Turkey, reinforced concrete is a widely used structural material in civil engineering. The main reasons for the widespread use of reinforced concrete are that the materials that make up the concrete and the reinforcement are easy to find and cheaper than other construction techniques.

The reinforced concrete used in buildings has two main functions: To transfer horizontal and vertical loads. Its first task is to transfer the horizontal loads acting on the support system, particularly those due to wind and seismic loads, to the vertical support elements together with the floors. The second is to transfer the dead and live loads transferred from the floor and the wall loads, if any, with columns or shears. In addition, through this transfer, the vertical members share the loads in proportion to their stiffness. Under this heading, reinforced concrete beams are mentioned.

Pure bending is a state of stress in which only bending moment is applied to a beam without axial, shear or torsional forces. In a beam under pure bending, the neutral axis from the stress direction divides the section into two regions. Compressive stresses occur in one region and tensile stresses in the other.

There will be no cracks in the beam at very low load values. Under the effect of increasing loads, the first crack will occur when the unit strain in the outermost tensile fiber reaches the unit strain limit of the concrete in tension. However, cracking is generally defined as the concrete in the outermost fibre reaching the tensile strength in flexure, based on strength rather than deformation.

Reinforcement should be used to encounter these tensile stresses. The amount, ratio, position and arrangement of the reinforcement to be placed in the beam will change the behaviour of the beam depending on the applied load. Beam sections are divided

into two classes as single and double reinforced sections, depending on the calculations made according to the reinforcements in the compression and tension zone. It is assumed that in single-reinforced sections, the longitudinal reinforcement is located only in the tensile region of the section, while in double-reinforced sections, the longitudinal reinforcement is in both tension and compression regions.

In general, as a result of the conditions imposed on longitudinal reinforcement in the (*TS500*, 2000) and (*Türkiye Bina Deprem Yönetmeliği*, 2018), it is obligatory to have a certain amount of longitudinal reinforcement in both tension and compression zones along the beam.

However, since it is the simplest reinforced concrete section calculation, single-reinforced section calculations are examined. This calculation is also considered as the neglect of the contribution of the reinforcement in the compression zone to the bearing capacity.

2.2. Failure on the RC Beam

Horizontal load-bearing systems, such as beams and floors in reinforced concrete structures, tend to bend due to the vertical loads applied. In addition to the bending effect, shear and torsion effects also occur in this type of member.

Bending moment, shear force, torsional moment and normal force can occur depending on the way the beams are supported and also depending on the loading. Firstly, the behaviour of reinforced concrete sections under the action of bending (simple bending condition) is briefly mentioned.

In those members that attempt to bend, part of the member section is subjected to tensile stress and part to compressive stress. By placing reinforcement on the tensile stressed parts of such elements, the tensile strength of the section is increased. This also allows the concrete in the compression zone to work at full capacity.

2.2.1. Flexural failures

Experimental studies have shown that reinforced concrete sections subjected to axial compression (column) with simple bending (beam) or bending reach their fracture position by crushing the concrete in the outermost fibre. At the time of crushing, the concrete in the outermost compression fibre reaches εcu unit shortening. When this

position is reached, it is extremely important in terms of behaviour whether the tensile reinforcement yields or not. Accordingly, there are three types of failure in reinforced concrete.

- Balanced Failure
- Flexural Compression Failure
- Flexural Tension Failure

2.2.1.1. Balanced failure

In the fracture position, the crushing of the concrete in the outermost fiber and the yielding of the tension reinforcement occur simultaneously. This type of fracture is called balanced fracture. Balanced fracture determines the upper limit of tensile fracture and the lower limit of compression fracture. No or very insufficient steel: Steel suddenly overexpands, breaks and concrete is crushed. As soon as the steel yield, the concrete is crushed by shortening $\varepsilon_{cu} = 0.003$. In this type of fracture, almost no cracks are seen since the steel does not have a chance to extend further after yielding. This type of fracture also has the following characteristics.

- It is a type of fracture between tensile fracture and compression fracture.
- When the steel yields, $\varepsilon_s = \varepsilon_{sd}$

2.2.1.2. Flexural compression failure

In this fracture location, the concrete is crushed before the reinforcement reaches its yield point. The stress that occurs in the reinforcement is smaller than the available strength and strain per unit elongation corresponding to flow. Unit shortening reached maximum unit shortening in concrete. Steel stretches very little, it does not bend. No cracks occur or are too capillary to be seen. The concrete gradually gets shorter, the unit shortening reaches $\varepsilon_{cu} = 0.003$ and the concrete is crushed. The fracture is dominated by the properties of concrete. It is a sudden and brittle fracture. A beam equipped in this way means there is too much reinforcement. This type of fracture also has the following characteristics.

When the stress on the reinforcing bar is in the $(\varepsilon_s < \varepsilon_{sd})$ state, the concrete reaches its limit state.

It is the most dangerous form of fracture.

It does not give any symptoms; it suddenly collapses as a sound like an explosion sound.

There is no time to take action and evacuate the structure.

2.2.1.3. Flexural tension failure

At the moment of failure ($\sigma_s < f_{yd}$) and ($\varepsilon_s < \varepsilon_{sy}$), tensile reinforcement yields first, then the outermost concrete compression fiber is crushed. As the steel continues to yield, crushing occurs in the concrete. The stresses in the concrete gradually increase and reach the limit state. As soon as the limit is reached, crushing begins in the concrete. The property of the steel dominates the fracture and the fracture shows a ductile behaviour. In this case, the relationship of the element (Moment- Curvature) is similar to the elasto-plastic ($\sigma - \varepsilon$) diagram of steel. This fracture is ductile and is called ''Tensile Failure''. This type of fracture also has the following characteristics.

- Ductile fracture is not instantaneous.
- There are extreme cracks and displacements for a while before it collapses.

It allows time to evacuate the building as it prevents the sudden breakage of the concrete by prolonging, since the steel yield first. Therefore, this type of fracture is desirable.

When the fracture types are examined, ductile fracture is a preferred behaviour in civil engineering. Since a structural element with a brittle behaviour will suddenly break without showing any stimulating deformation, it is not possible to take precautions or empty the structure before it collapses. The following recommendations should be considered to ensure ductile behaviour.

- The conditions of (*TS500*, 2000) and (*Türkiye Bina Deprem Yönetmeliği*, 2018) must be strictly fulfilled.
- Columns should be confined from the foundation to the roof, including the beam joints.
- At the ends of the beams and columns, close confinement should be used (stirrups, spirals) and the ends of the stirrups and spirals should be inserted into the concrete core.
- Care should be taken to clamp the reinforcements and deformed concrete reinforcing bar should be used.

2.2.2. Shear failures

In cross sections, axial force and bending moment create normal stress, while shear force and torsion moment create shear stress. Depending on the loading in the beams, the value of the shear force changes along the beam length. The fracture form of a beam, which is also under the influence of shear force, is quite complex; It varies depending on the loading, the distance of the load from the support, the depth of the beam, the concrete compressive strength, and the amount and arrangement of the tension and shear reinforcements. The cracks occurring in the selected continuous beam as an example are given schematically.

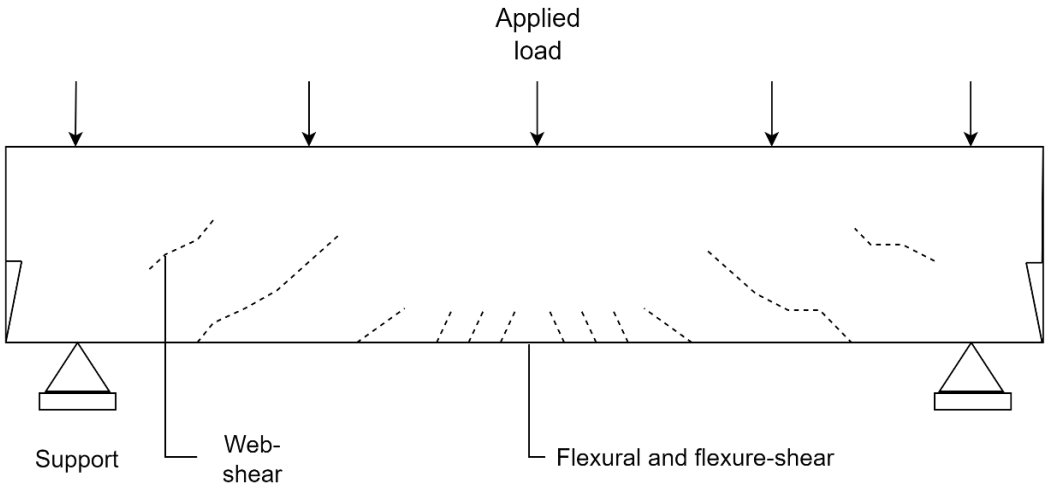

Figure 2.1. Schematic view of cracks in continuous beam (Doğangün, 2019)

Shear cracking occurs in the neutral axis region of the beam and does not reach the lower and upper surfaces of the beam. The crack that reaches the outermost concrete fiber in the tensile zone on the lower surface of the beam is not a shear crack, but this crack is called an oblique crack. For a crack to qualify as an oblique crack, the crack must be oblique across the depth of the beam and cause a stress spike in the tensile reinforcement. The stress that causes this crack is also defined as oblique tension.

2.2.2.1. Bearing capacity of the elements under the shear effect

Elements that make up the reinforced concrete structure generally carry shear forces in addition to bending. Since the shear strength of concrete is quite high compared to its tensile strength, shear fractures are not common in reinforced concrete elements. On the other hand, principal tensile stresses caused by shear and normal stresses cause significant problems due to the tensile strength of concrete. Since the shear and

compressive strength of concrete is higher than the tensile strength, even in the case of simple slips (basit kayma), breakage occurs due to principal tensile stresses.

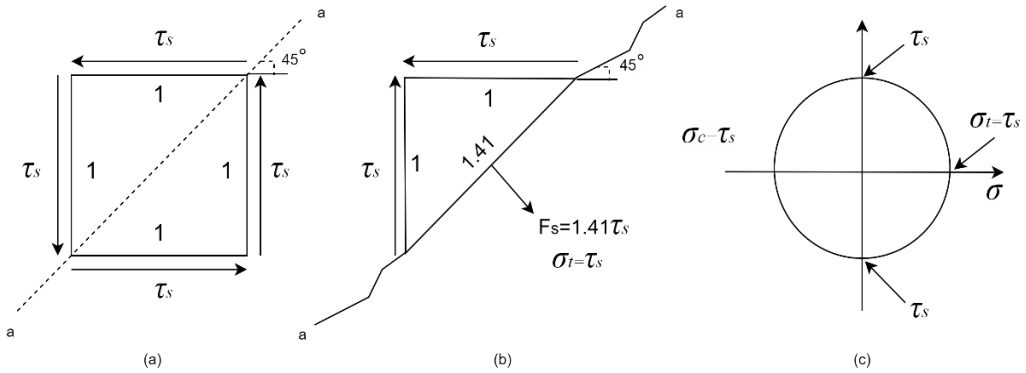

Figure 2.2. Principal stresses under simple shear (Ersoy et al., 2012)

In the case of simple shear, the principal tensile and compressive stresses will be equal to the shear stress, and fracture will occur due to the lowest strength, tensile. Since the principal tensile stresses will act on a plane that makes an angle of 45 degrees to the surface on which the shear stress acts, the fracture will occur with an oblique crack formed in the direction perpendicular to the principal tensile stresses.

Such oblique cracks due to principal tensile stresses are extremely dangerous and can cause brittle fracture. In cases where normal stresses act with shear, the slope of the oblique crack depends on the direction of the principal tensile stresses.

At the neutral axis level, the normal stresses are zero, and the cracking occurs at an angle of 45 degrees to the beam axis. Since cracking occurs perpendicular to the principal tensile stresses, the slope of the oblique crack extending from the lower face of the beam to the upper face decreases. Oblique cracks, which cause major problems in reinforced concrete and cause brittle fracture, are caused by principal tensile stresses, not shear stresses.

It was suggested for the first time by Ritter that shear stresses do not cause problems in reinforced concrete elements, and that their cracking and fracture is caused by the principal tensile stresses that occur with the contribution of these stresses. Then, oblique cracking and fractures caused by shear forces were investigated by Mörsch. In the calculation method proposed by Mörsch, shear stresses are taken as basis instead of principal tensile stresses.

A cracked reinforced concrete section is considered for the calculation of shear stresses.

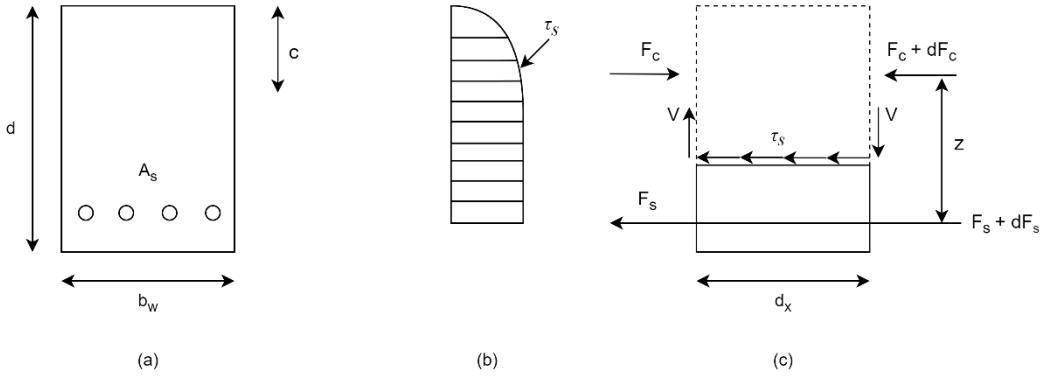

Figure 2.3. Assumptions in Mörsch theory(Ersoy et al., 2012)

$$\tau_s . b_w . d_x + F_s = F_s + d . F_s \tag{2.1}$$

$$\tau_s . b_w . d_x = d . F_s = dM/z \tag{2.2}$$

$$\frac{dM}{d_x} = V \tag{2.3}$$

$$\tau_s' = \frac{V}{b_w} . z \tag{2.4}$$

$$z \approx 0.9\, d \tag{2.5}$$

$$\text{Unit coupling force; } \frac{d_s}{d_x} D \tag{2.6}$$

$$\tau_s = \frac{V}{0.9 . b_w . d} \tag{2.7}$$

2.2.2.2. Beams without shear reinforcement

TS 500 (TS500, 2000)and Turkey Building Earthquake Code (Türkiye Bina Deprem Yönetmeliği, 2018) require a minimum level of shear reinforcement, no matter how small the shear stresses. However, in order to understand the beam behaviour, it is important to understand the behaviour of the beam without shear reinforcement.

The beams in the Figure 2.4 are simply supported beams without shear reinforcement. It will be assumed that there is only tension reinforcement in the beam that extends from the support to the support and is clamped there on the lower surface. Where a = shear span ; d = depth ratio , one of the most important parameters affecting the beam shear behaviour is the ratio of shear span to depth ratio (a/d).

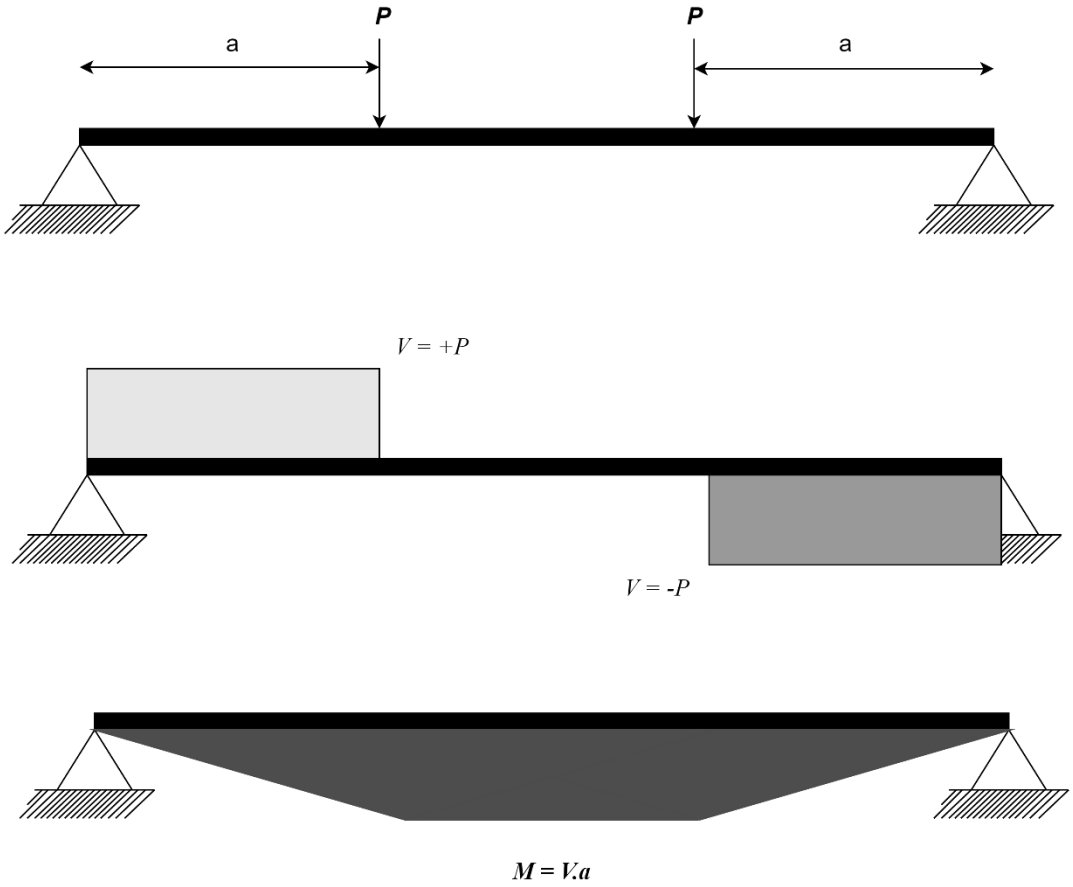

Figure 2.4. Beam without shear reinforcement and resulting section effects (Doğangün, 2019)

One of the most important parameters affecting the beam shear behaviour is the ratio of shear span to depth ratio ($\frac{a}{d}$). How this ratio changes the beam behaviour is given below.

- $\left(\frac{a}{d}\right)$ > 7, The beam usually achieves its bearing strength by bending fracture. Shear force has no effect on fracture. Oblique cracks do not occur in this type of beam.

- $3 < \left(\frac{a}{d}\right) < 7$, While crack progress follows 1, 2, and 3 in theFigure 2.5, an oblique crack, indicated as 4, occurs suddenly. When this crack occurs, there is a complete "oblique crack" situation. When this stage is reached, a sudden jump in the elongation of the tensile reinforcement is observed. Inclined crack, the crack must be oblique across the depth of the beam and cause a stress spike in the tensile reinforcement. This jump indicates a "stress fit" caused by oblique cracking. Here, the fracture load and the load at which the oblique crack occurs are the same.

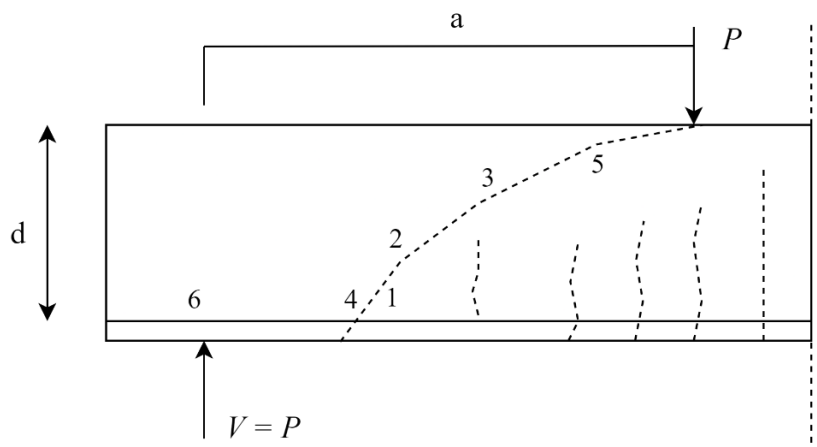

Figure 2.5. Oblique Crack Formation (Ersoy et al., 2012)

- $1.5 < \left(\frac{a}{d}\right) < 3$, shear-pressure (shear-crush) fracture. Here, the fracture load is greater than the cracking load. The 1, 2, 3 cracks to be noted here is not "oblique cracking".

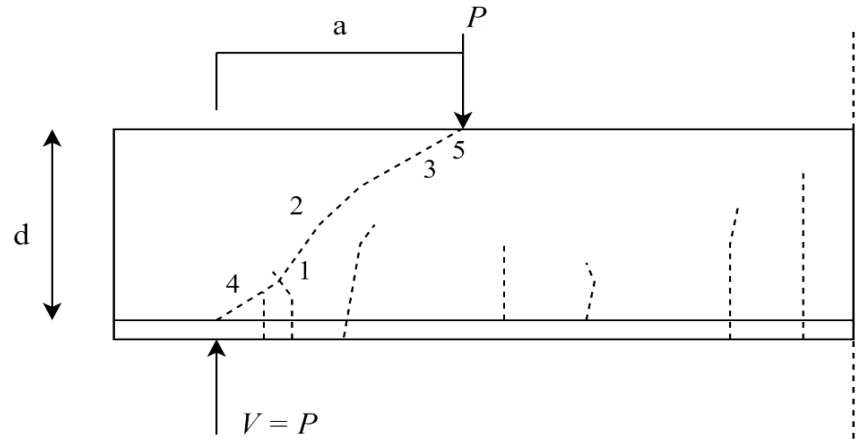

Figure 2.6. Formation of Oblique Cracks (Ersoy et al., 2012)

- $\left(\frac{a}{d}\right)$ < 1, In cases where the shear distance is very small, the bending loses its significance after the oblique crack has formed and the beam now behaves completely like a tensioned belt. Here, the reinforcement yields before the beam reaches the breaking position, that is, the beam reaches its bending capacity. Fracture occurs in two ways.

a. Crushing of the body due to compressive stresses (Marked as 1 and 2 in the Figure 2.6)

b. The absence of clamping beyond the support due to high stresses in the reienforcement during the transfer of pressure

In addition, tensile cracks may occur on the upper face of the beam as a natural consequence of the tensioned belt behaviour. Such a crack is shown in the Figure 2.7.

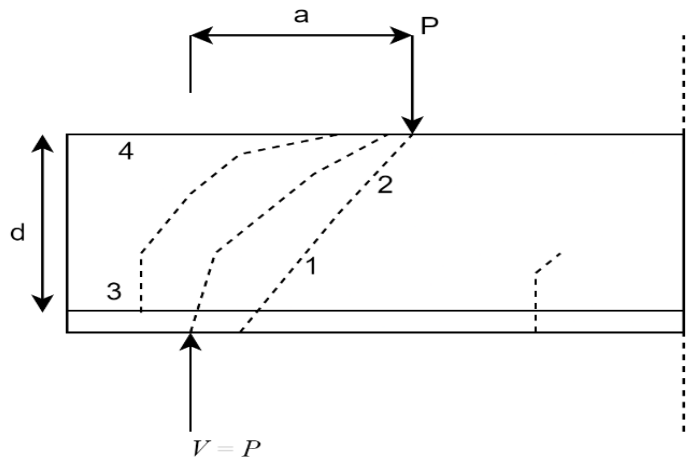

Figure 2.7. Formation of Oblique Cracks (Ersoy et al., 2012)

In a beam without shear reinforcement and inclined cracks, the shear effect is compensated by the 3 internal forces V_{cc}, V_{cd} and V_{ci}.

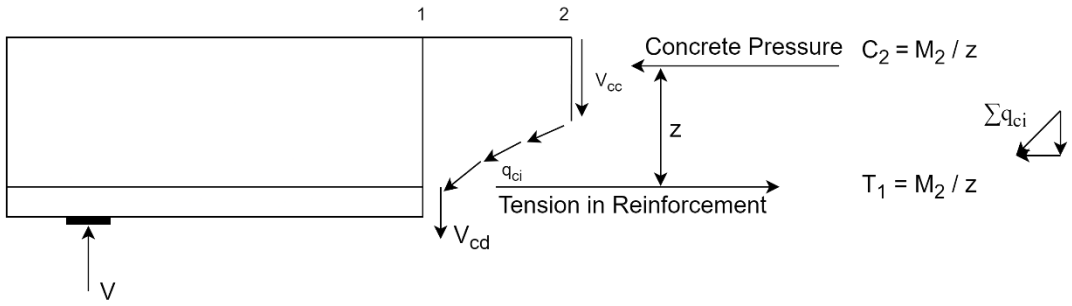

Figure 2.8. Transfer of shear force in reinforced concrete beam(Ersoy et al., 2012)

V_{cc}: Shear force carried in the uncracked pressure zone (Concrete admixture = %20-40)

V_{cd}: Shear force carried by tensile reinforcement (leverage effect of longitudinal reinforcement = 15-25%)

q_{ci}: In-crack shear stresses,

V_{ci}: The vertical resultant of the sum of the in-crack shear stresses shown as q_{ci}, (Contribution of friction = 33-50%)

Equilibrium equation for forces in the vertical direction,

$$V = V_{cc} + V_{cd} + V_{ci} \tag{2.8}$$

2.3. Code Review

The following section summarizes the shear design provisions in TS500, Eurocode 2 and ACI 318 used to estimate shear capacities.

2.3.1. TS500

In the TS500 regulation, V_r is the shear strength of the section. The shear strength of the section is obtained by adding the concrete contribution (V_c) and the shear reinforcement contribution (V_w). The contribution of concrete is calculated from Equation (2.11). The shear cracking strength of a reinforced concrete section can be calculated using the following equation.

$$V_r \leq V_d \tag{2.9}$$

$$V_r = V_c + V_w \tag{2.10}$$

$$V_c = 0.8\, V_{cr} \tag{2.11}$$

$$V_{cr} = 0.65\, .\, f_{ctd}\, b_w\, d \tag{2.12}$$

$$V_w = \frac{A_{sw}}{s}\, f_{ywd}\, d \tag{2.13}$$

2.3.2. Eurocode 2

The Shear resistance of a beam member with shear reinforcement is equal to V_{Rd}. In the case of an inclined compression chord , V_{ccd} is the design value of the shear component of the force in the compression area. V_{td} is the design value of the shear component of the force in the tensile reinforcement, in the case of an inclined tensile chord.

$$V_{Rd} = V_{Rd,s} + V_{ccd} + V_{td} \tag{2.14}$$

$$V_{Rd,s} = \frac{A_{sw}}{s} z f_{ywd} \cot\theta \tag{2.15}$$

f_{ywd} should be set to 0.8. $\cot\theta$ varies according to countries. The suggested range for this expression is given below.

$$1 \leq \cot\theta \leq 2{,}5 \tag{2.16}$$

2.3.3. ACI 318

$V_c$is the shear strength provided by concrete, and V_s is the shear strength provided by the shear reinforcement. V_n, obtained by the sum of V_c and V_s, is multiplied by the strength reduction factor to keep the calculation on the safe side.

$$\Phi V_n \geq V_u \tag{2.17}$$

$$V_n = V_c + V_s \tag{2.18}$$

$$V_c = 2\sqrt{f'_c}\, b_w\, d \tag{2.19}$$

$$V_s = \frac{A_v f_y d}{s} \tag{2.20}$$

As seen in the formulas above, TS500 and ACI 318 regulations are similar. That's why the results are close.

2.4. Review of Related Work

Shear cracking in reinforced concrete elements and control of this cracking has been tried to be calculated for decades. The correct calculation and prevention of this damage is very important. Because, as civil engineers, our expectation from reinforced concrete elements is that the type of damage is realised at once, giving people the time to escape in disasters such as earthquakes.

In order to better understand shear damage in reinforced concrete beams, reinforced concrete beams without shear reinforcement are analysed.(Kim & White, 1991; Sato et al., 2004) In 1995, (Ueda et al., 1995) developed a new truss model. With this model, they tried to explain the shear resistance in shear reinforced concrete beams. Many researchers have worked to better understand the shear failure mechanism and diagonal shear failure in reinforced concrete members (Adebar & van Leeuwen, 1999; De Silva et al., 2005; Witchukreangkrai, 2004; Witchukreangkrai et al., 2006; Zakaria et al., 2009; Zararis, 2003).

Zakaria et al. experimentally studied 10 simply supported beam specimens with constant width b = 200 mm. The characteristic strength of concrete was fc = 40 MPa and the largest aggregate size was 25 mm. All specimens were tested on a 5000 kN test machine with monotonic point loading. The shear reinforcement thickness used in the tests was 10 mm. As a result of his experiments, it was observed that the shear crack width, the strain of the shear reinforcement and the gap between the shear cracks gradually increased. In addition, the test results revealed that longitudinal reinforcement and shear reinforcement are very important against diagonal crack gap and opening. The experimental results were found suitable for the development of a shear crack displacement prediction method (Zakaria et al., 2009).

In the experimental study conducted by (Słowik, 2014); 6000 kN monotonic load was applied to a beam with 13 longitudinal reinforcements and no shear reinforcement. Surface displacement gauges and observation were used to measure crack formation. The beams have a rectangular surface area with total depth h = 0.25 m, width b = 0.12 m and effective depth d = 0.22 m. 5 beams with a length of 2.05 m were subjected to 4-point bending test. Since the shear span to depth ratio is different for each beam, the distance between the applied loads is different for each beam. Since the beams are of the same concrete class, the compressive and tensile strengths are the same. Young's

modulus = 41400 MPa, Fc = 35 MPa and Fct = 3.5 MPa. The largest aggregate size is 16 mm. Longitudinal reinforcements are 2 deformed steel bars of 18 mm. The yield strength of the steel is fy = 453 Mpa and tensile strength ft = 698 MPa. As a result of the study, diagonal shear failure was found to cause a size effect. It was also understood that the size effect is that the ultimate shear capacity decreases as the depth of the beam increases. The tests performed in this study showed that the effective length - depth ratio affects the shear resistance and maximum shear capacity.

2.5. Finite Element Modeling

The Finite Element Method (FEM) is a numerical solution method that provides realistic solutions to many engineering problems with an acceptable approach. FEM was first applied to vibration systems by Courant in 1943 (Courant, 1943). In this method, the system is divided into small elements, each of which is calculated in its own sub-solution domain. These finite elements are connected by nodes and can be 1, 2 or 3 dimensional. This makes it much easier to solve complex engineering problems (Demir, 2018).

ABAQUS is a software package that works with the finite element model and aims to give realistic results for computer-aided engineering problems. Different material models and finite element types are included in the library. It offers the possibility to analyse linear and non-linear problems that are difficult to solve. It consists of five software packages. ABAQUS CAE was used in this study (H. Hibbitt et al., 2013).

3. MATERIAL AND SIMULATION

3.1. Methodology

The finite element method (FEM) is one of the numerical solution methods that produces realistic solutions to many complex problems with the developing computer technology. In this method, the system is divided into small finite elements and each of these divided elements is solved in itself. FEM is frequently used for modeling reinforced concrete elements. However, in order to obtain correct results while modeling, the material model must be chosen correctly and modeled correctly. In the study carried out within the scope of this thesis, the ABAQUS program, which works with the finite element method, was used (Demir, 2018).

3.1.1. Element types

Having a wide variety of elements in the element library of the ABAQUS program provides flexibility in modeling different geometries and structures. Elements are characterized by type, number of nodes, degrees of freedom, formulation and integration. Commonly used element types are shown in the Figure 3.1.

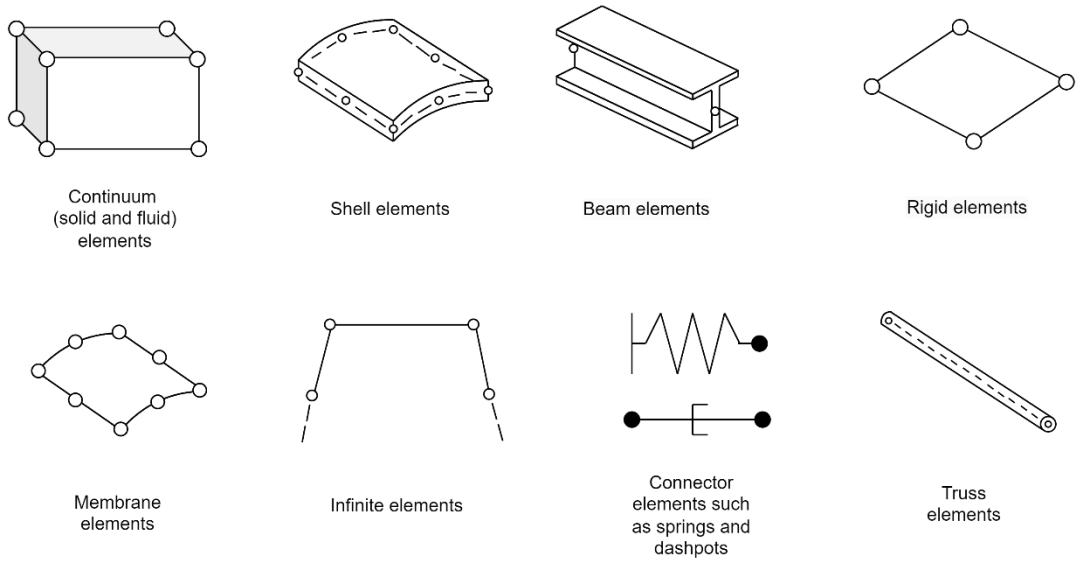

Figure 3.1. One, two and three dimensional finite elements (H. Hibbitt et al., 2013)

A solid element has linear and quadratic interpolation in the program according to the number of nodes. The elements are called linear if they only have nodes at the corner points, and they are called quadratic elements if there are node points in the middle of these nodes. At the same time, there are full house reduced integration elements in the program.

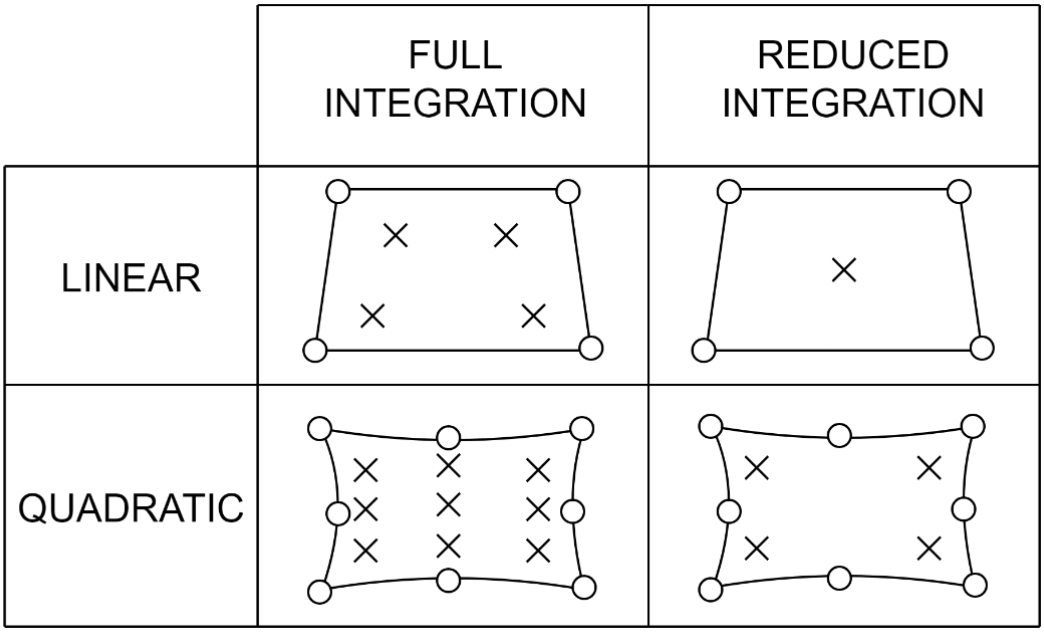

Figure 3.2. Elements with full and reduced integration (Demirtaş, 2019)

The element mass and stiffness are calculated numerically at the integration points. This numerical algorithm determines how the element will behave. The reduced integration uses fewer rows of integration to establish the stiffness of the element and shortens the analysis time (K. Hibbitt & Karlsson, 2013).

In this thesis, continuum solid is used in the solid elements library to model the concrete material. The beam element is used to define the reinforcement material. A rigid element is used to prevent the bearing and load plates from being loaded and to transfer the incoming load.

3.1.2. Concrete material model

There are two concrete material models in ABAQUS. These are concrete damage plasticity and concrete smeared cracking. A concrete damage plasticity material model was used to accurately describe the nonlinear behavior of concrete. This model considers isotropic damage elasticity including isotropic tensile and compressive

plasticity. In addition, the CDP model takes into account the reduction in elastic stiffness due to plastic strains under compression and tension (H. Hibbitt et al., 2013). The CDP model was first proposed by (Lubliner et al., 1989) for monotonic loading. It was later developed by (Lee & Fenves, 1998) to take into account dynamic and cyclic loading effects (Demir, 2018). It uses the damage parameter as an internal variable, together with its elastoplastic behavior under compressive and tensile stress, to characterize the inelastic behavior of concrete material (Demirtaş et al., 2018).

There are two failure mechanisms to describe the concrete material pattern: compression crushing and tensile cracking. As seen in the Figure 3.3, the behavior of the CDP model under uniaxial tension is defined by the linear elastic stress-strain relationship until the concrete reaches the maximum tensile stress (σ_{t0}) value. Tensile cracking manifests in concrete upon reaching the critical stress threshold. The region characterized by diminishing strength due to crack propagation is termed as tensile stiffness, which can be quantified through a declining stress-strain correlation or fracture energy expression (Earij et al., 2017).

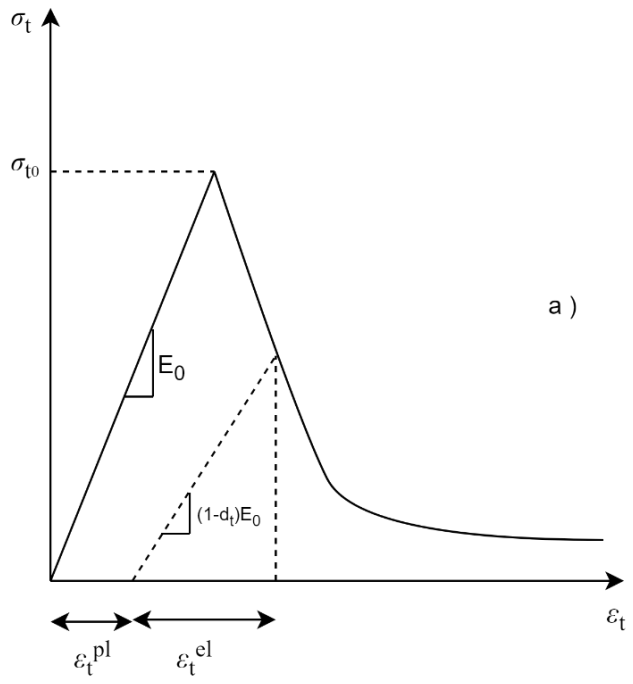

Figure 3.3. Tensile behavior of concrete (H. Hibbitt et al., 2013)

During uniaxial compressive loading, the CDP model exhibits linear behavior until reaching the critical stress, σ_{c0}. Once this strength threshold is surpassed, plastic deformations initiate in the concrete. The response within the range of $\sigma_{c0}$and ultimate

compressive strength, σ_{cu}, is characterized as strength hardening, while the behavior following the exceedance of σ_{cu} is denoted as strength softening (H. Hibbitt et al., 2013).

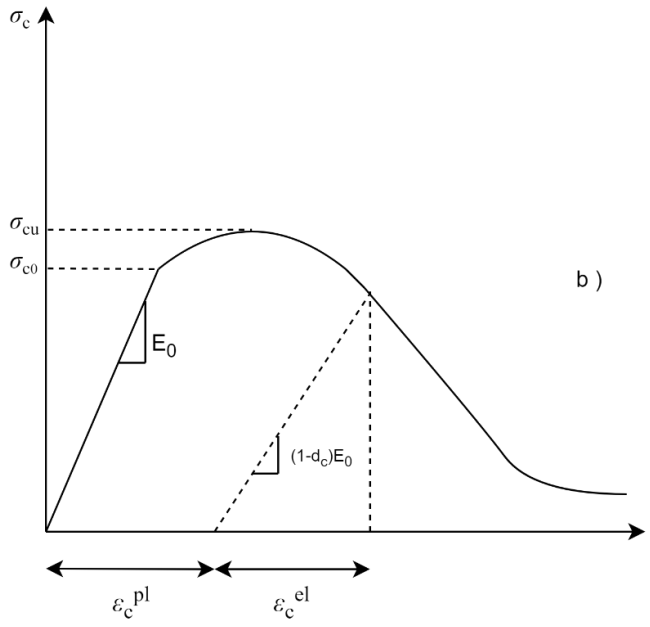

Figure 3.4. Compressive behavior of concrete (H. Hibbitt et al., 2013)

$\varepsilon_c^{\sim pl}$: Plastic deformation under compression

ε_c^{in} : Inelastic deformation under compression

$\varepsilon_t^{\sim pl}$: Plastic deformation under tension

ε_t^{ck} : Inelastic deformation under tension

E_0 : Initial modulus of elasticity

The relationship between stress and strain is expressed in Equations 1 and 2 depending on these parameters.

$$\sigma_c = (1 - d_c).E_0.\left(\varepsilon_c - \varepsilon_c^{\sim pl}\right) \quad (3.1)$$

$$\sigma_t = (1 - d_t).E_0.\left(\varepsilon_t - \varepsilon_t^{\sim pl}\right) \quad (3.2)$$

The fracture surface is controlled by two variables $\varepsilon_t^{\sim pl}$ and $\varepsilon_c^{\sim pl}$, which depend on the fracture mechanism under compressive and tensile loading. Concrete stress-strain

behavior can be obtained by experimental studies or models given in the literature (Mander et al., 1988).

The obtained stress - strain ($\sigma - \varepsilon$) values should be entered to the program as stress - inelastic strain ($\sigma - \varepsilon_c^{in}$). The entered values are automatically converted to stress - plastic strain ($\sigma - \varepsilon_c^{pl}$). values by the program. The relation between these values is defined by Equation 3.3 - 3.6.

$$\varepsilon_c^{in} = \varepsilon_c - \frac{\sigma_c}{E_0} \tag{3.3}$$

$$\varepsilon_c^{\sim pl} = \varepsilon_c^{in} - \frac{d_c}{(1 - d_c)} \cdot \frac{\sigma_c}{E_0} \tag{3.4}$$

$$\varepsilon_t^{ck} = \varepsilon_t - \frac{\sigma_t}{E_0} \tag{3.5}$$

$$\varepsilon_t^{\sim pl} = \varepsilon_t^{\sim ck} - \frac{d_t}{(1 - d_t)} \cdot \frac{\sigma_t}{E_0} \tag{3.6}$$

d_c and d_t are damage parameters expressing the decrease in elastic stiffness of concrete under the effect of compressive and tensile stresses, and are expressed by equations 3.7 and 3.8. Damage parameter value varies between 0 and 1. 0 means no damage, 1 means fully damaged.

$$d_c = 1 - \frac{\frac{\sigma_c}{E_0}}{\frac{\sigma_c}{E_0} + \varepsilon_c^{in}(1 - b_c)} \tag{3.7}$$

$$d_t = 1 - \frac{\frac{\sigma_{t0}}{E_0}}{\frac{\sigma_{t0}}{E_0} + \varepsilon_c^{ck}(1 - b_t)} \tag{3.8}$$

$$b_c = \frac{\varepsilon_c^{pl}}{\varepsilon_c^{\sim in}} \tag{3.9}$$

$$b_t = \frac{\varepsilon_t^{pl}}{\varepsilon_t^{\sim ck}} \tag{3.10}$$

3.1.3. Concrete cracking energy criterion

The behavior that goes beyond the elastic limit with the formation of cracking in concrete under uniaxial tension is modeled by the "tensile softening" behavior, also known as "tensile stiffness", which models the stress transfer between concrete and reinforcement. The behavior of concrete under tensile stress can be defined as stress - crack width or stress – strain (Demirtaş et al., 2018).

Defining tensile stiffness as a stress-strain curve can create a convergence problem in the model in case of absence or low reinforcement. This problem usually occurs when the crack is localized in one area. The area under the stress - crack width curve is expressed as fracture energy. Three different models have been proposed in the literature to describe the tensile strength - crack width curve.

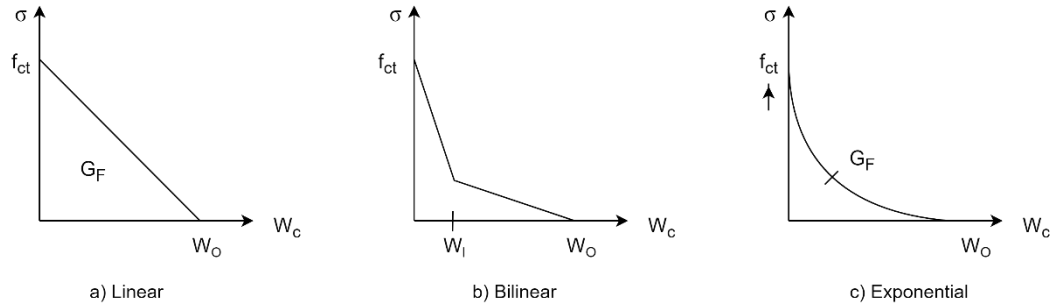

Figure 3.5. Tensile behavior of concrete after cracking (Demir et al., 2016)

The simplest approach to describe the behavior is the linear tensile stiffness model. This model gives reasonably accurate results, but the response of concrete tends to be quite rigid. Instead, a bilinear or exponential approach is used to describe the descending portion of the stress-strain curve (Earij et al., 2017).

3.1.4. Yield fuction

The elastic limits under possible stress combinations in concrete are determined by a yield surface. The yield surface envelope under plane stress used in the CDP model is also given in Figure 3.6.

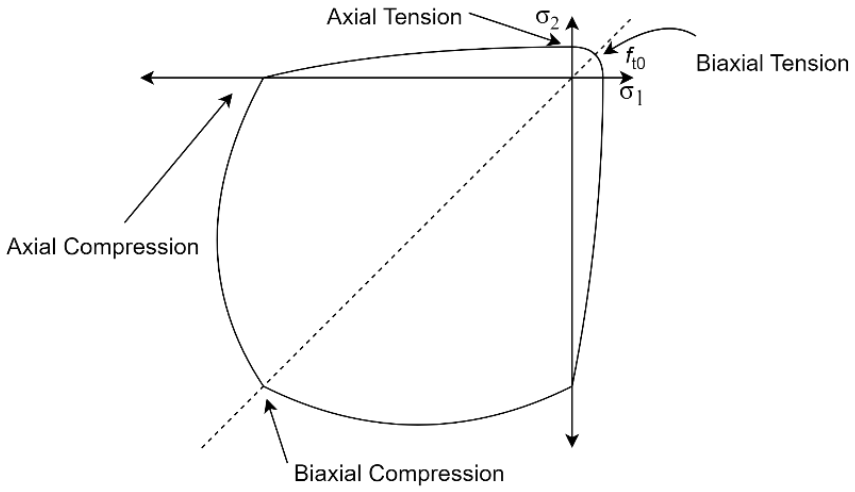

Figure 3.6. Biaxial stress force fatigue envelepo of concrete (Sümer, 2010)

The parameters required to form the yield surface of the concrete are the ratio of the biaxial compressive yield stress to the uniaxial compressive stress ($\frac{\sigma_{b0}}{\sigma_{c0}}$), the eccentricity parameter (ε), the dilation angle (ψ), and the secondary constant stress ratio on the tensile function (K_c). The default value for the eccentricity parameter (ε) is given as 0.1 in the program. ($\frac{\sigma_{b0}}{\sigma_{c0}}$) takes values between 1.10 and 1.16 (Lubliner et al., 1989). In this study, this value was taken as 1.16. The default value for the kc value is ($\frac{2}{3}$) given. The dilation angle (ψ) represents the plastic volumetric change. Parametric studies are required to determine the dilation angle realistically (Demir, 2018). As a result of the parametric studies carried out within the scope of this thesis, this value was taken as 20.

Material models that exhibit stress and stiffness reduction often create convergence problems in analysis. To overcome this convergence problem, viscoplastic arrangement is made. With the definition of viscoplasticity, convergence is achieved by ensuring that the stresses are slightly outside the yield surface. The default value of the viscosity parameter is given as 0 in the ABAQUS program. A value of 0 means no viscoplastic regulation (K. Hibbitt & Karlsson, 2013). As a result of the parametric studies carried out within the scope of this thesis, this value was taken as 0.0025.

3.1.5. Plastic yield potential

The plastic yield potential is defined by the relationship between stress and plastic strain. For this, the Drucker - Prager function given in the equation below is used.

$$G = \sqrt{(\epsilon . \sigma_{t0} \tan\psi)^2 + \bar{q}^2} - \bar{p} . \tan\psi \qquad (3.11)$$

Table 3.1. Drucker-Prager function parameters

Symbols	Despcription
ϵ	Yield surface eccentricity
ψ	Dilation angle
σ_{t0}	Axial tension stress
$\bar{q}$	Equivalent mises effective stress
$\bar{p}$	Hydrostatic compressive stress

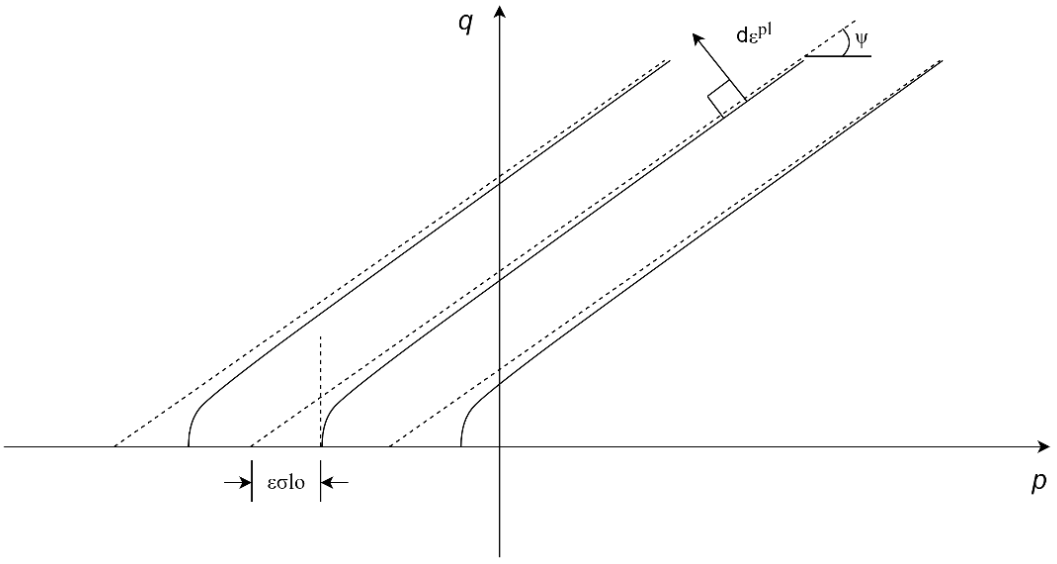

Figure 3.7. Drucker-Prager hyperbolic function (Sümer, 2010)

3.1.6. Reinforcement material model

The material behavior of reinforcing steel is defined in the literature as stress - strain. Embedded models are generally used in complex problems with a large number of elements. In the embedded model, the reinforcement is modeled using bar elements such as truss or beam and embedded in the concrete. In this study, the reinforcement is modeled as a beam and is assumed to be embedded in the concrete. The reason for modeling like this is that the increase in stirrup thickness cannot be observed when the truss element is used. Therefore, beam element model should be used in models with increased stirrup thickness.

The material model proposed by (Mander et al., 1988) in the literature was used to describe the stress-strain curve of the reinforcement. The equations necessary to describe the behavior are given below.

Table 3.2. Yield strength calculation of reinforcing steel

Elastic loading	$(0 \leq \varepsilon_s \leq \varepsilon_y)$	$f_s = E_s \,.\, \varepsilon_s$
Yield Zone	$(\varepsilon_y \leq \varepsilon_s \leq \varepsilon_{sh})$	$f_s = f_y$
Strength hardening	$(\varepsilon_{sh} \leq \varepsilon_s \leq \varepsilon_{su})$	$f_s = f_{su} + (f_y - f_{su}) \left\lvert \frac{\varepsilon_{su} - \varepsilon_s}{\varepsilon_{su} - \varepsilon_{sh}} \right\rvert^p$

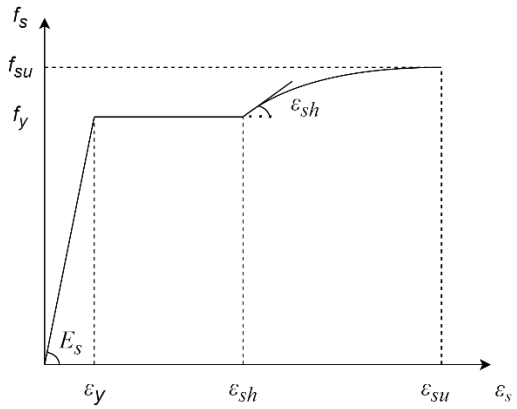

Figure 3.8. Reinforcement stress-strain diagram(Mander et al., 1988)

3.2. Experimental

In this section, detailed information is given about the article used in the analytical study and the experiments performed in the article used in this thesis. The behaviour of beams as transverse reinforcement under monotonous loading has been experimentally investigated. These reinforced concrete beams have rectangular section and continuous rectangular spiral reinforcement. An advanced rectangular spiral reinforcement consisting of shear-favourably inclined vertical joints was tested as shear reinforcement for shear-critical beams. It is possible to clearly see in the test results that the use of rectangular spiral reinforcement provides improved bearing capacity and improved shear performance in the beams studied.

In this article of Karayannis, eight (8) reinforced concrete beams were produced and tested (Karayannis & Chalioris, 2013). Although it is made for continuous rectangular spiral reinforcement, two (2) common closed stirrups beams (ST80,ST120) within 8 beams are considered in this thesis.

3.2.1. Characteristics of the tested beams

Both beams have similar properties as shown in Figure 3.9. Their total length is 1840 mm, the shear span is a = 720 mm, and the height to the width ratio is $\frac{h}{b}$ = 300/200 mm. The span to depth ratio equals to $\frac{a}{d}$ = 2.67 for both beams. The longitudinal reinforcements are 4 pieces of 18 mm in diameter, and the top 2 longitudinal reinforcements are 14 mm in diameter. The lower and upper longitudinal bars are hooked upwards and downwards beyond the supports.

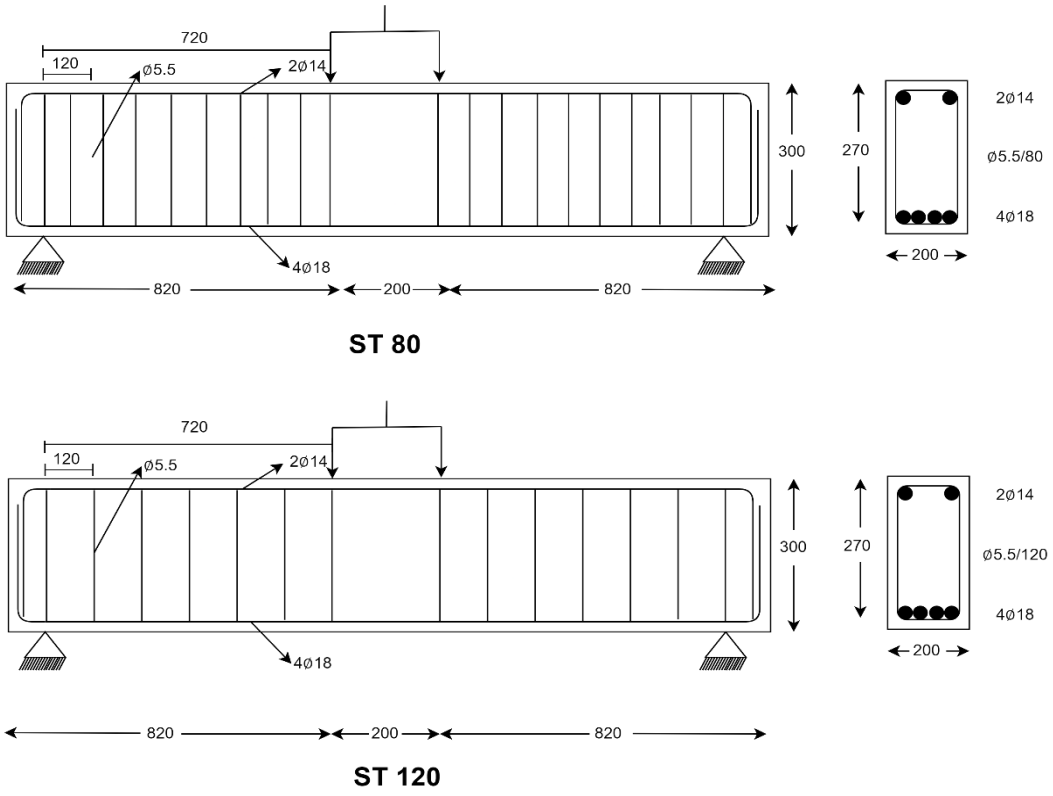

Figure 3.9. Geometry and steel reinforcements of the tested beams(Karayannis & Chalioris, 2013)

Yield and ultimate tensile strength of 18 mm steel reinforcements were measured and f_{yl} = 550 MPa and f_{ul} = 690 MPa were calculated, respectively. The flexural tension reinforcement ratio pl, and compression reinforcement ratio p_l', the values of the transverse reinforcement ratios, p_t is calculated using the following expressions.

$$p_l = \frac{A_{sl}}{bd} \tag{3.11}$$

$$p'_l = \frac{A'_{sl}}{bd} \tag{3.12}$$

$$p_t = \frac{A_{st}}{bs} \tag{3.13}$$

$$A_{st} = 2(\pi \frac{\emptyset_t^2}{4}) \tag{3.14}$$

In these formulas, b width and d effective depth of the cross section of the beam, A_{st} is the area of the two-legged stirrup, $\emptyset_t$ is the reinforcement diameter, s is the uniform

spacing of the shear reinforcement and also A_{sl} and A'_{sl} are the area of tension steel reinforcement and compression steel reinforcement, respectively. The stirrups used in the experiments are 5.5 mm thick. The yield tensile strength (f_{yt}) was 310 MPa and the ultimate tensile strength (f_{ut}) was 430 MPa.

The common features of the concretes produced within the scope of the experimental study are 10% fly ash, sand with high fineness coefficient, crushed stone aggregate with a maximum size of 32 mm and Greek type pozzolan cement containing water at a ratio of 1:2.27:3.15:0.54. In addition to these, 0.5 liter retarder was added for each cubic meter of concrete. Concrete samples were subjected to compression and tensile tests and were measured as $f_c = 28.5$ MPa and $f_{ct} = 2.60$ MPa.

3.2.2. Test equipment and instrumentation

A typical four-point bending scheme and setup was used for shear tests. Beams were simply edge-supported on roller supports 1640 mm apart using a rigid laboratory frame. In the middle of the beams, a load was applied to two points with 200 mm intervals using a steel spreader beam.

The load applied to the beam was increased continuously by a small amount using a fixed-end actuator and was measured by a load cell with an accuracy equal to 0.05 kN. Three LVDTs were used in the experiments and these instruments measure with an accuracy of 0.01 mm. One of these tools is placed in the middle span and the other two are placed on the supports. Load and deflection measurements up to the ultimate bearing capacity of the beams were continuously read and recorded during the experiments.

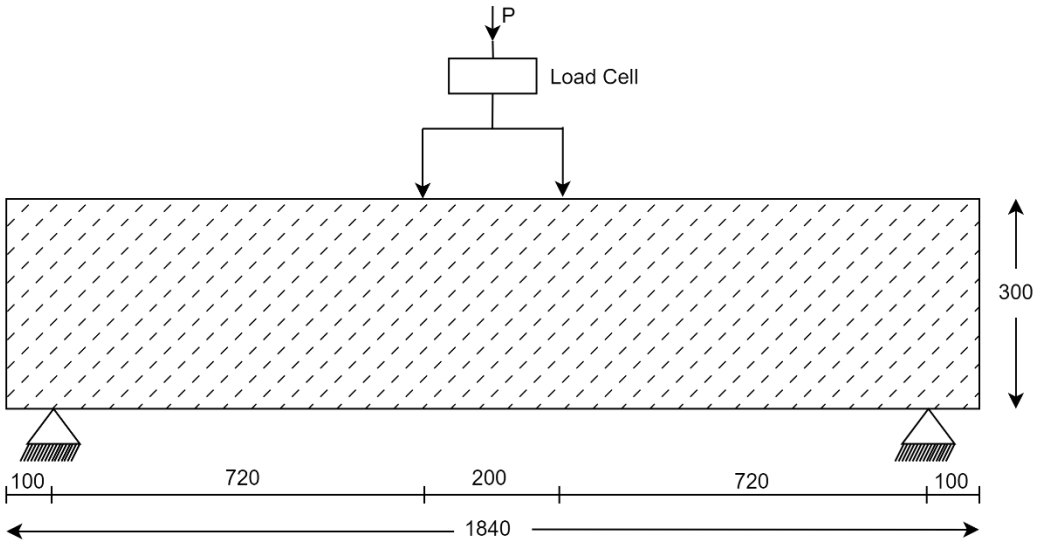

Figure 3.10. Test rig and instrumentation (Karayannis & Chalioris, 2013)

3.2.3. Experimental test results

Maximum measured value of applied load, PMax, the corresponding ultimate shear strength, $\left(Vu = \frac{P_{max}}{2}\right)$and average shear stress, $\left(\upsilon_u = \frac{V_u}{b.d}\right)$ along with the corresponding deformation at the maximum (peak) load, δ_{peak} of all the tested beams are presented in Table 3.3

Table 3.3. Test Results

Beam Name	$\boldsymbol{\frac{a}{d}}$	$\boldsymbol{p_l}$ **(%)**	$\boldsymbol{p_t}$ **(%)**	$\boldsymbol{P_{max}}$ **(kN)**	$\boldsymbol{V_u}$ **(kN)**	$\boldsymbol{\upsilon_u}$ $\boldsymbol{(MPa)}$	$\boldsymbol{\delta_{peak}}$ **(mm)**
ST80	2.67	1.885	0.297	251.0	125.5	2.32	7.30
ST120	2.67	1.885	0.198	215.0	107.5	1.99	7.59

3.3. Numerical Modeling

In this section, the analysis results of beams modelled with the ABAQUS finite element program and their comparison with the test results will be given.

First, the concrete, reinforcement, load and support plates that make up the model are modelled in the "part" module of the program. Concrete and reinforcements were created using 3D solid and beam elements, respectively. The load and support plates

are then formed as 3D analytical rigid elements. In the Property module, parameters such as density of the material, Young's modulus, poisson's ratio are defined. The created parts are combined in the assembly module. The reinforcements were placed in the concrete, and the load and support plates were placed on the upper and lower surfaces of the sample in the same way as in the experimental setup. The reinforcements are modelled as embedded in the concrete, and the bond boundary condition is defined for the surfaces between the load and support plates and the concrete. In the load module, the support conditions of the model, one of which is fixed and the other is movable, are created on the support plates. The applied load is defined on the load plate as level displacement.

In the numerical model, concrete 8-node linear brick, incompatible modes (C3D8I) elements and reinforcement bars are modelled with 2-node linear beam in space (B31) finite elements. In order to determine the optimum mesh size of concrete, a parametric study was carried out and as suggested in the literature, mesh sizes of 20, 25 and 50 millimetres were tried parametrically, with an aspect ratio of 1. Obtaining the results of each model made in the optimum time while choosing the mesh size is also discussed. Technical specifications of the modeled computer; 2.9 GHz processor speed, 16 gb ram and GTX 1650 graphics card. Since the reinforcements are modelled as beam elements, they are divided into the same mesh size as the concrete in one direction only. Since the reinforcements are modelled as beam elements, they are divided into the same mesh size as the concrete in one direction only. A FE model created for the samples used in the experimental study and the model divided into solution networks are shown in the Figure 3.11.

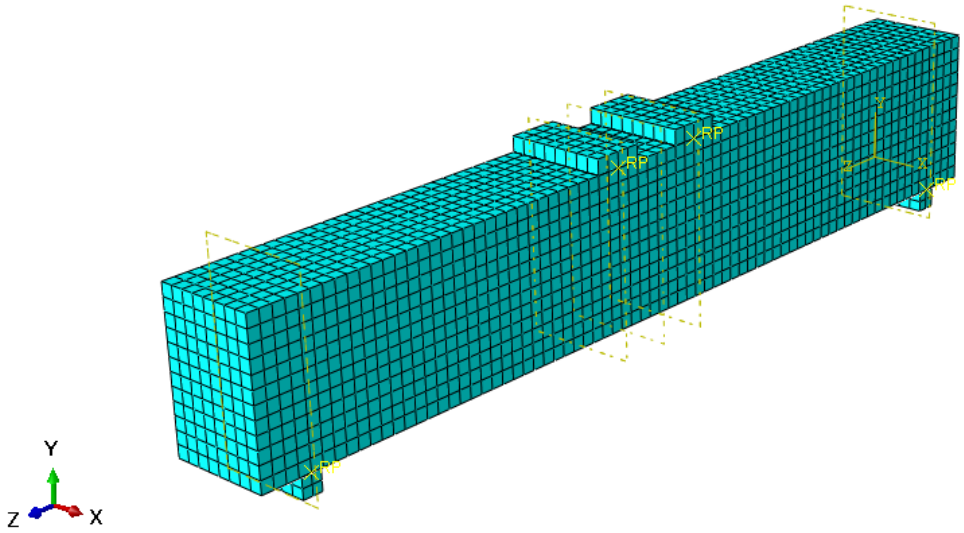

Figure 3.11. Sample FE Model

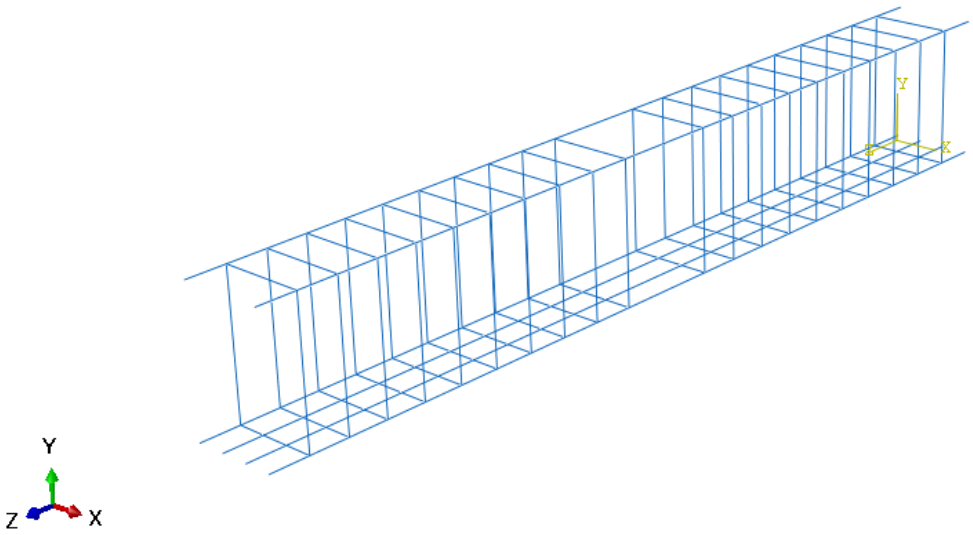

Figure 3.12. Reinforcement Model Sample

The material properties of reinforced concrete beams, supports and steel reinforcements are calculated according to the standards specified in ACI and the values are defined to the elements modelled under the property module using the SI unit system. In this study, in addition to the material properties of concrete and steel elements, the 'Concrete Damaged Plasticity Model', which defines the beam behaviour specified in the ABAQUS user manual, is based. The parameters that are dependent on this model are given in the Table 3.4 below.

Table 3.4. CDP Model Parameters

Parameter	Value
ψ	20
ε	0,1
$\sigma_{b0} / \sigma_{c0}$	1,16
K	0,6667
μ	0,0025

The behaviour of concrete under pressure is defined in terms of stress - elastic strain (σ_c - ε_c^{in}), and the behaviour under tension in terms of stress - crack strain (σ_t - ε_{cr}) in Figure 3.13. In addition, graphs showing the behaviour of the damage parameter under compression and tension are shown in Figure 3.13 and Figure 3.14.

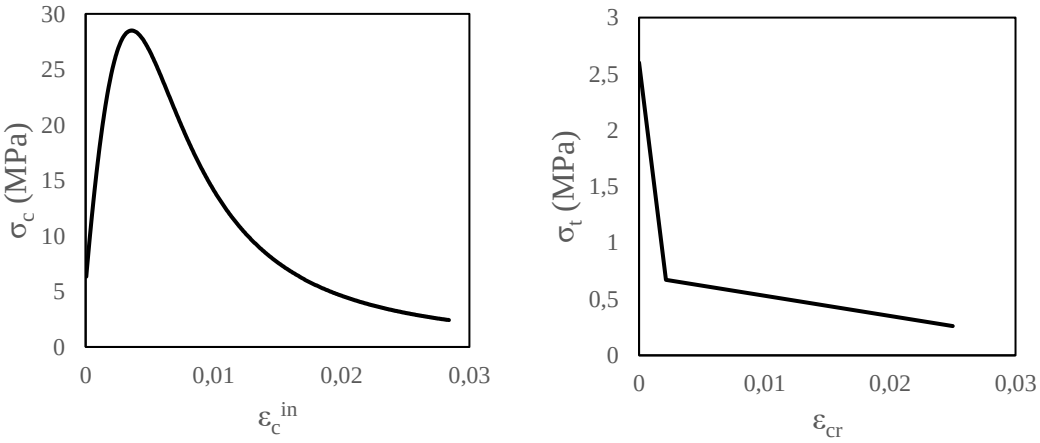

(a) (b)

Figure 3.13. Constituve modal graph of concrete under compression (a) and tension (b)

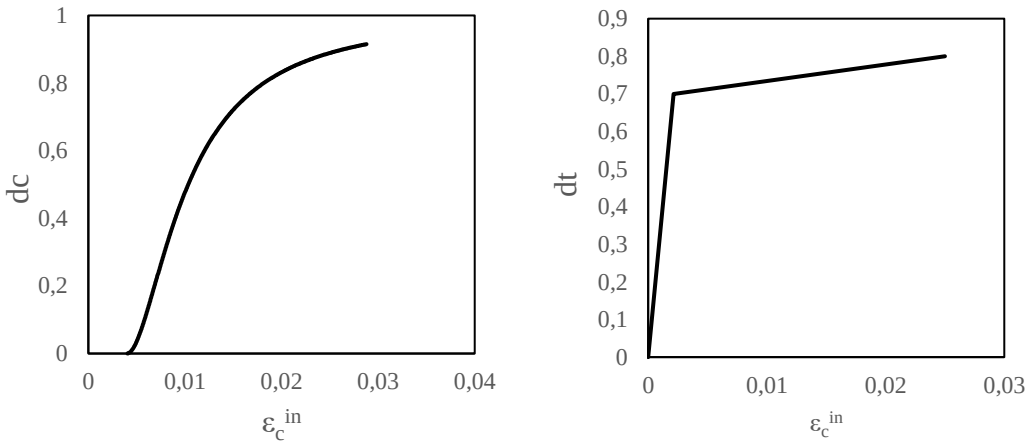

(c) (d)

Figure 3.14. Graphs of damage parameters of concrete under compression (a) and tensile (b) effects

Concrete samples were subjected to compression and tensile tests and were measured as $f_c = 28.5\ MPa$ and $f_{ct} = 2.6\ MPa$. The value of fc is known in the table, and other parameters were determined based on this value by using numerical calculation methods given in the literature.

Table 3.5. Other parameters used in the numerical model of concrete

Parameter	**Value**
E	29153
Poisson's ratio	0.2
Density (g/cm^3)	2.4

It is defined as the material behavior ($\sigma_s - \varepsilon_s^{pl}$) of the reinforcing steel in the FE model. An example curve ($\sigma_s - \varepsilon_s^{pl}$) defined in the numerical model is shown in the Figure 3.15. Since different steel properties are not specified for Ø14 and Ø18 rebars, the data in Table 3.6 for both are entered.

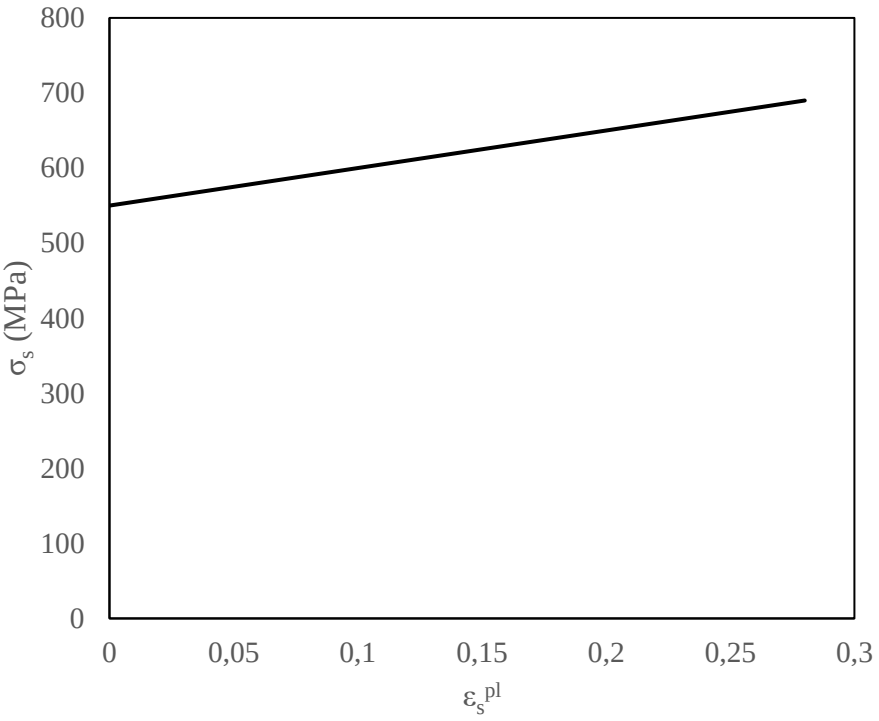

Figure 3.15. Reinforcing steel behaviour chart

Table 3.6. Ø14 and Ø18 steel reinforcement properties

Parameter	**Value**
E	200000
Poisson's ratio	0.3
Density (g/cm^3)	7.85

After the defined material properties, the elements were transformed into volumetric form in the "Assembly" module with the help of the coordinate plane. One at the midpoint of the upper plates and the lower supports are defined as the reference point. Thanks to this point on the upper plates, the load transfer of the rigid plates to the beam is ensured.

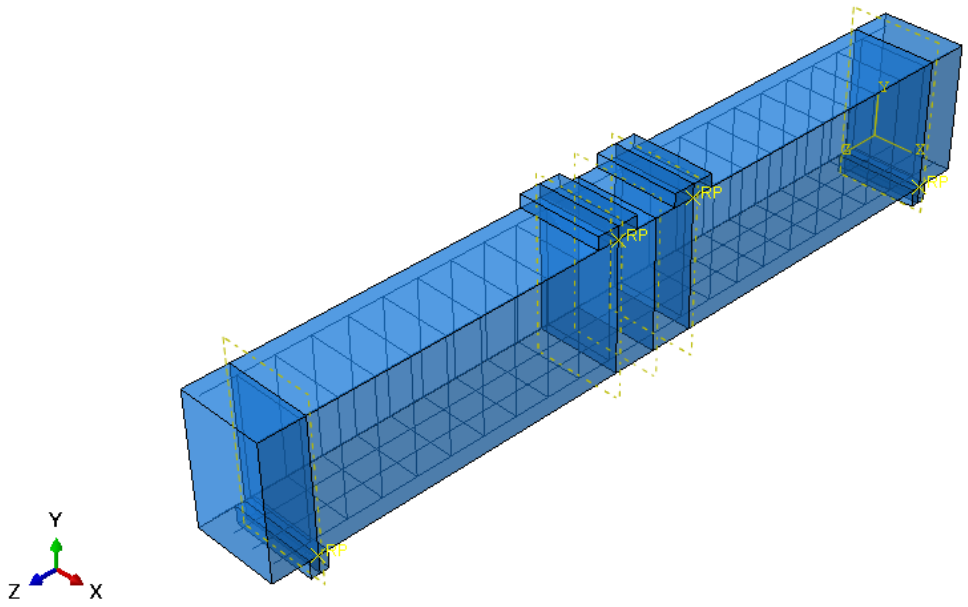

Figure 3.16. Assembly module

In order for the surfaces in contact with each other to move realistically in harmony, some constraints must be defined in the program. Selected "general contact(standard)", which allows to impose restrictions for all surfaces in contact with a single command. Normal behavior and tangential behavior are selected for Contact properties. After tangential behavior selection, friction coeff value of 0.25 was taken. "Hard" Contact is selected for normal behavior. In addition, "Embedded Region" was chosen so that the reinforcements remain embedded in the concrete. The load was given from the top two plates. For the finite element model, the structural meshing process has been carried out. Square finite element meshes with a size of 50 mm were created. The sliding support used in the experiment was chosen as the support condition.

After the completion of the numerical model, the validation of the model was determined by comparing the "load – mid point displacement" behavior graphs obtained from the Karayannis experiment results with the results of the FE model.

3.4. Calibration Process

3.4.1. Mesh sensivity

One of the most important parameters when it is desired to perform analysis in programs using finite element modeling is element size. Because if the element size is

not selected optimally, it can change the accuracy of the results. In this thesis, element sizes of 20, 25 and 50 mm were tried to find the optimum mesh size.(Tatar et al., 2017).

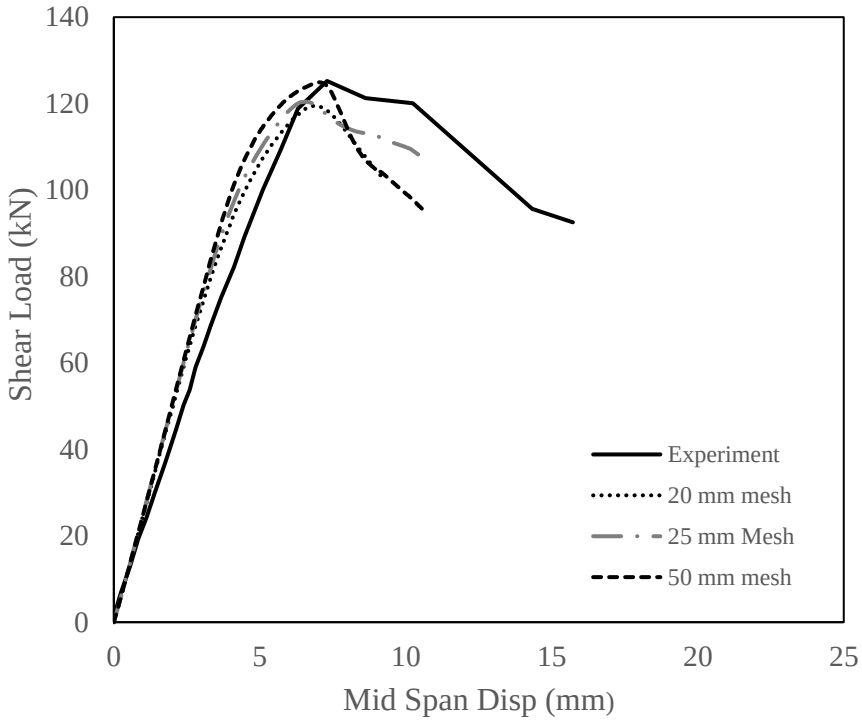

Figure 3.17. Element Size Sensivity Analysis

As shown in Figure 3.17, as a result of the parametric study, it has been seen that the optimum mesh size is 50 mm, as it gives both closer and faster results

3.4.2. Beam-Truss difference

In the first models created to investigate the shear damage of a reinforced concrete beam, Truss (T3D2) was chosen as the element type. This element type represents a linear 3D truss with 2 nodes. However, with this selection, although the stirrup size in the beams increased, the force received by the stirrup remained the same.

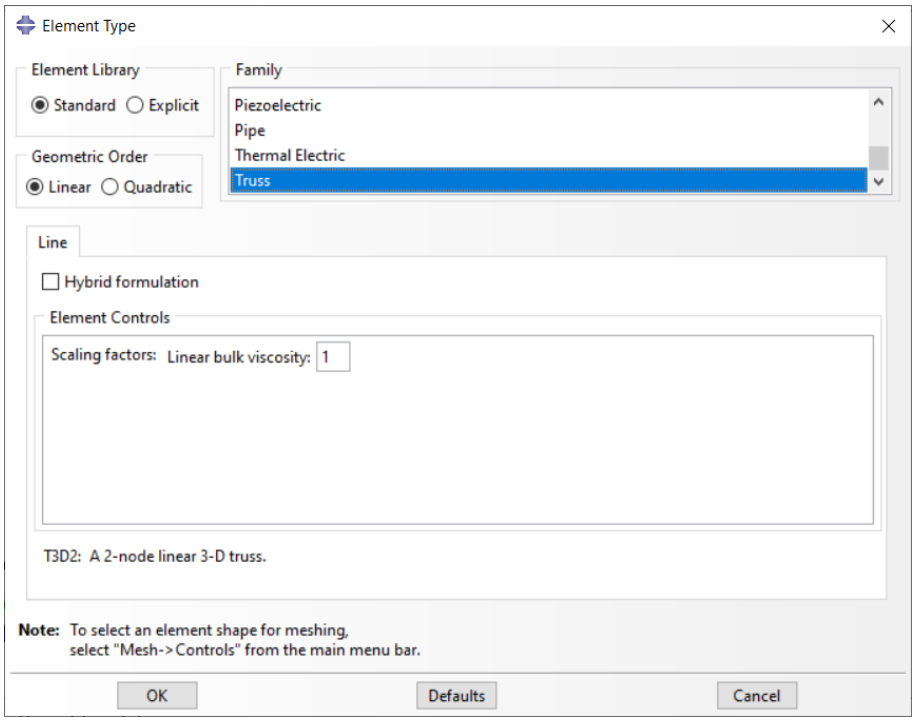

Figure 3.18. Truss element type

In the subsequent models, Beam (B31) was selected as the element type to reflect the force taken by the stirrup more accurately to the model. This model represents a linear beam with 2 nodes in space.

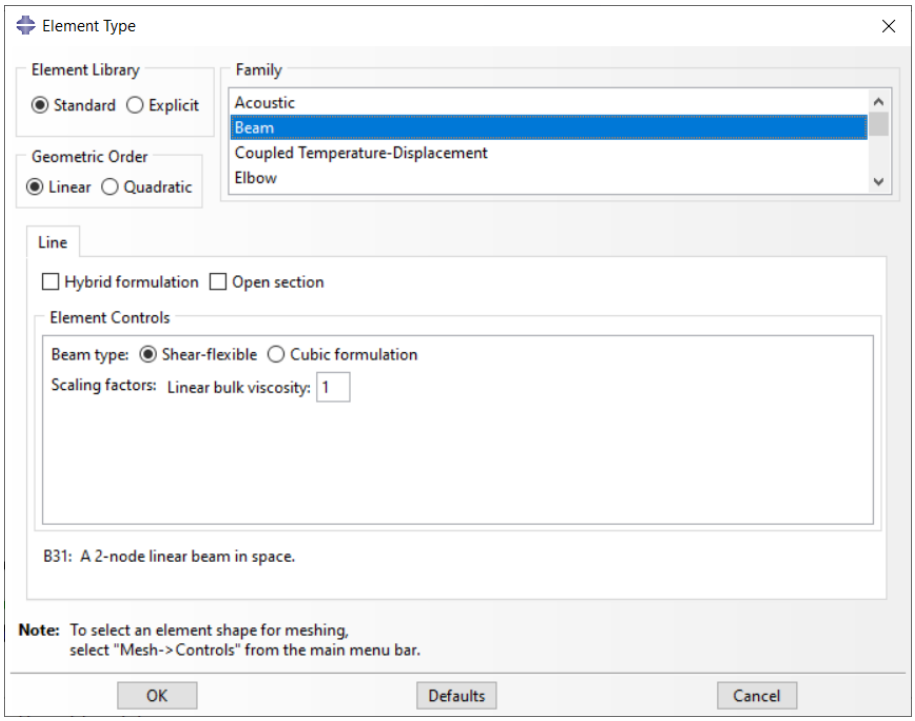

Figure 3.19. Beam element type

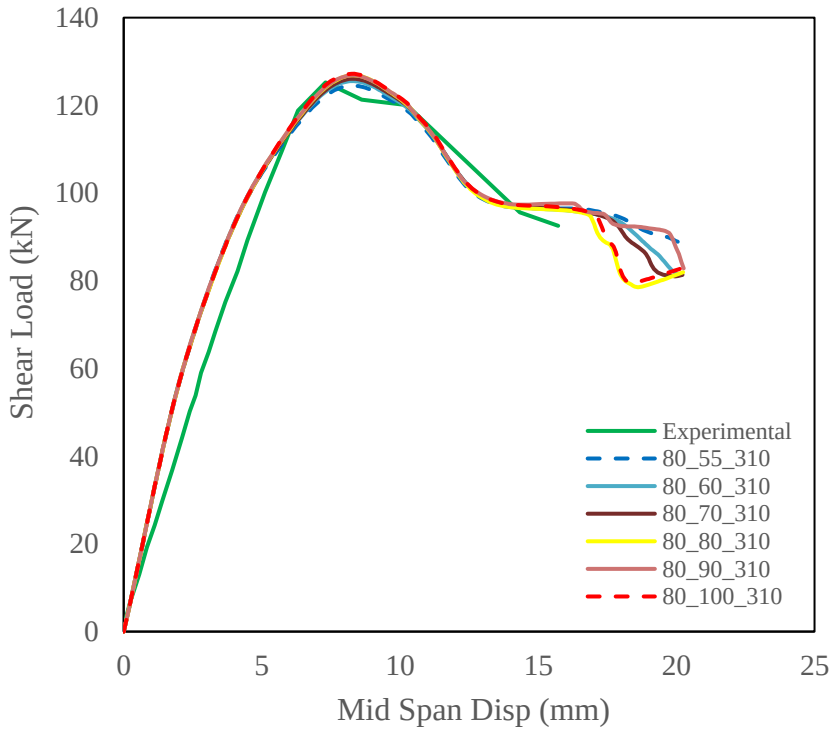

Figure 3.20. ST80 Truss Element Type Model

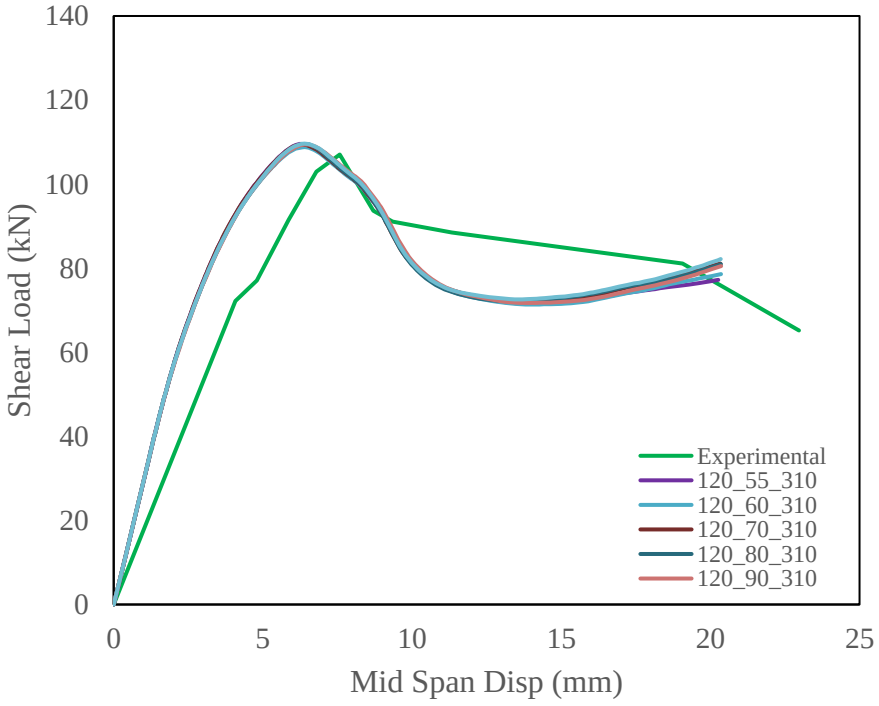

Figure 3.21. ST120 Truss Element Type Model

Figure 3.20 and Figure 3.21 show the results of 6 beams subjected to Karayannis test and parametric study in ABAQUS program. In the graphs, the shear damage in the center of the beam due to the change in stirrup thickness is measured. As seen in the graphs, it is not correct to model the shear damage using the truss element model in the finite element modeling method. The results are very close and scattered.

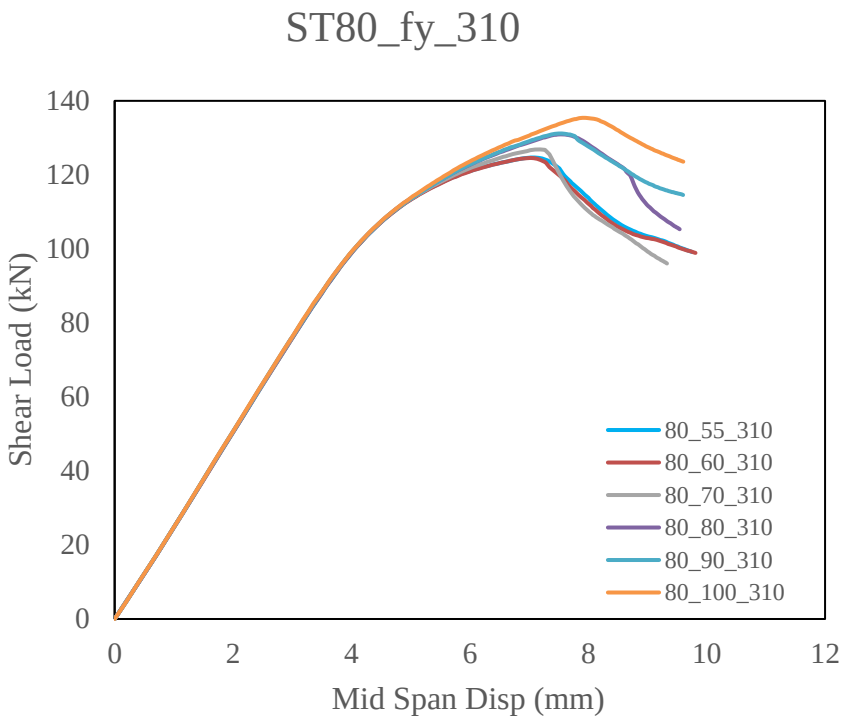

Figure 3.22. ST80 beam element type model results

As can be seen in Figure 3.22, when beam elements are used, the results do not overlap and the midpoint displacement and shear force received by reinforced concrete beams increase with the increase in stirrup thickness. For this reason, it is necessary to use beam elements in the models to be created.

3.4.3. Plasticity flow parameters

In the ABAQUS program, there are parameters that need to be entered to create the CDP model. These parameters are required to create the yield surface of the concrete. The dilation angle is very important to accurately model the stress-strain behavior of concrete in compression. For this parameter, it is stated in the literature that it is appropriate to take a value between 0 and 56. After hundreds of models, it was found that the most accurate value for the dilation angle in this thesis is 20.

The values for yield surface eccentricity (ε), Ratio of initial axial compressive yield stress to initial axial compressive stress (σ_{b0} / σ_{c0}) and Secondary constant stress ratio on the tensile function (K) the values shown in the Table 3.7 in the literature are used.

Setting the viscosity parameter other than 0 means applying viscoplastic regulation to the material model. However, in the literature, if convergence cannot be achieved in the models, it is possible to determine the optimum value of the viscosity parameter specific to this thesis with a parametric study, taking into account the values recommended in the literature.

Therefore, parametric studies were carried out within the scope of this thesis and it was concluded that the optimum viscosity parameter is 0.0025.

Table 3.7. Parameters used for CDP

Parameter	**Description**	**Value**
ψ	Dilation Angle	20
ε	Yield surface eccentricity	0,1
σ_{b0} / σ_{c0}	Ratio of initial axial compressive yield stress to initial axial compressive stress	1,16
K	Secondary constant stress ratio on the tensile function	0,6667
μ	Viscosity parameter	0,0025

3.5. Parametric Study

When sufficient convergence is achieved in these two behaviors, it is accepted that the numerical model is confirmed and it has been decided that a parametric study can be performed on this model.

For the nomenclature of the beam models, the number at the beginning of the model represents the stirrup spacing. The middle number represents the stirrup thickness and the last number represents the yield strength of the shear reinforcement.

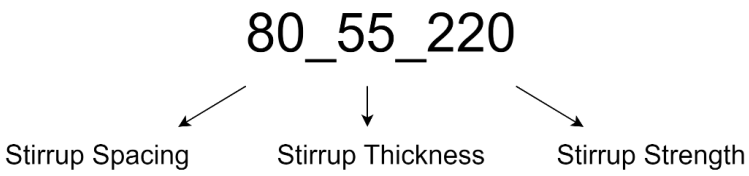

Figure 3.23. Sample string

Within the scope of this thesis study, 2 tested beams are considered. Similar size beams were designed with the specimens used in the experimental study. First, modeling was done for the beam in which the stirrups were installed at 80 mm intervals. Keeping the stirrup yield strength constant, 6 beam models were made for different stirrup thicknesses.

In this way, a total of 36 beams were modeled for different stirrup yield strengths. 18 of these models are for 80 mm stirrup spacing and 18 for 120 mm stirrup spacing.

Table 3.8. Parametric study of the beams and their properties

Sample Name	Stirrup Space (cm)	Stirrup Thickness (mm)	Stirrup Strength (MPa)
80_55_220	80	55	220
80_60_220	80	60	220
80_70_220	80	70	220
80_90_220	80	90	220

Table 3.8. (Continued) Parameters used for CDP

80_100_220	80	100	220
80_55_310	80	55	310
80_60_310	80	60	310
80_70_310	80	70	310
80_80_310	80	80	310
80_90_310	80	90	310
80_100_310	80	100	310
80_55_420	80	55	420
80_60_420	80	60	420
80_70_420	80	70	420
80_80_420	80	80	420
80_90_420	80	90	420
80_100_420	80	100	420
120_55_220	120	55	220
120_60_220	120	60	220
120_70_220	120	70	220
120_80_220	120	80	220
120_90_220	120	90	220
120_100_220	120	100	220
120_55_310	120	55	310

Table 3.8. (Continued) Parameters used for CDP

120_60_310	120	60	310
120_70_310	120	70	310
120_80_310	120	80	310
120_90_310	120	90	310
120_100_310	120	100	310
120_55_420	120	55	420
120_60_420	120	60	420
120_70_420	120	70	420
120_80_420	120	80	420
120_90_420	120	90	420
120_100_420	120	100	420

4. NUMERICAL AND PARAMETRIC STUDY RESULTS

4.1. Numerical Model Results

In this thesis, it is aimed to investigate the parameters affecting the shear capacity of reinforced concrete beams by numerical modeling method. For this purpose, 2 test specimens selected from the literature were modeled in ABAQUS, a finite element program. The results of the 2 models were consistent with the experimental results. According to this result, it was seen that the experiment can be created in a virtual environment. With the parametric study, the shear capacity of the beams and the limits of these parameters were investigated.

ST80 and ST120 beams were modeled in ABAQUS program. The experimental results and the results of the models are shown in Figure 4.1. It is possible to say that the results are consistent.

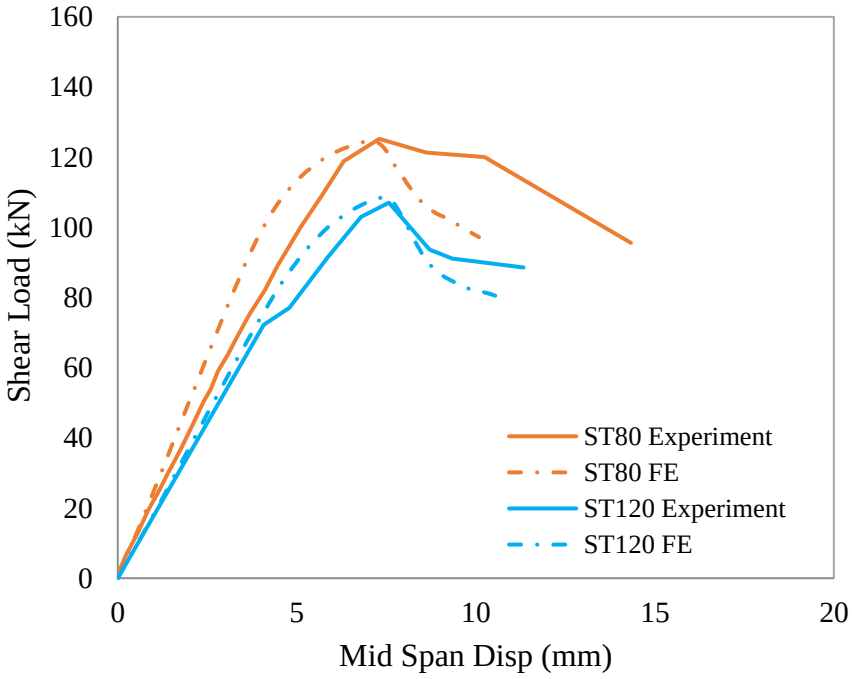

Figure 4.1. Experimental and FE behavioral models

4.2. Parametric Study Results

In this thesis, in order to investigate the parameters affecting the shear capacity of reinforced concrete beams by numerical modelling methods, the experiment was selected from the literature and modelled in ABAQUS software. During the experiment, it was observed that the amount of vertical and horizontal displacement of the specimens was kept at a limited level. The conditions of ST120 reinforced concrete beams before and after the experiment are given in the Figure 4.2 and Figure 4.3.

The results of the experimental study and the numerical modeling results were similar. A parametric study was performed by accepting the accuracy of the model. In this study, the stirrup spacing and shear reinforcement yield strength were kept constant and the results were obtained by varying the stirrup thickness.The condition of the reinforced concrete beam specimens modelled in ABAQUS programme after being subjected to the same loading as the experiment is shown in Figure 4.4

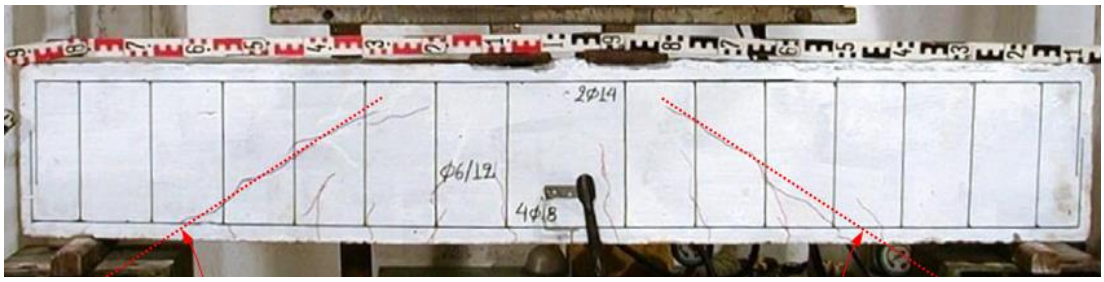

Figure 4.2. Pre-test condition of ST120 beam

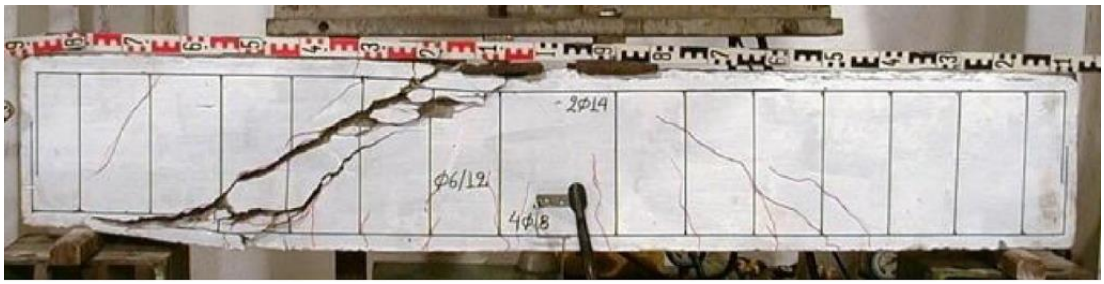

Figure 4.3. Damaged condition of ST120 beam after the test

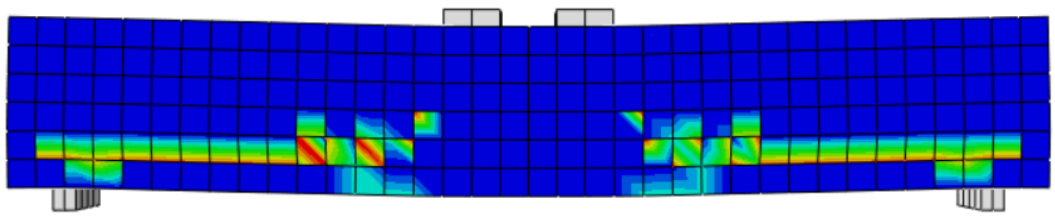

Figure 4.4. ST120 beam numerical analysis result

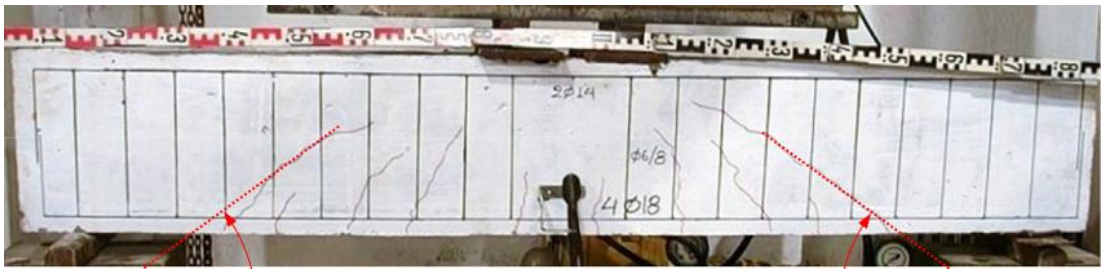

Figure 4.5. Condition of ST80 beam before the experiment

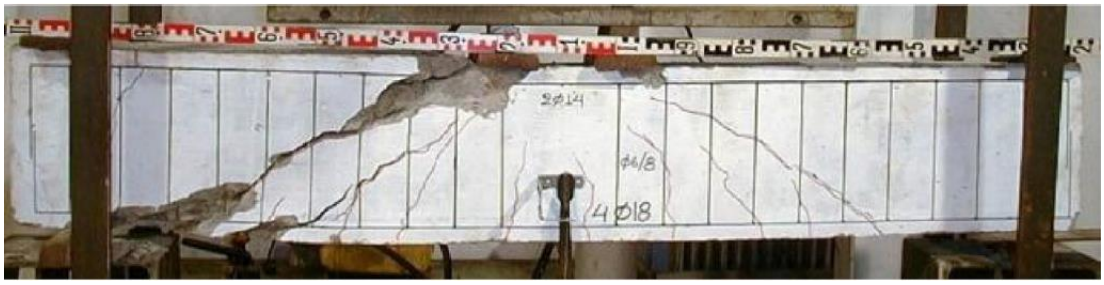

Figure 4.6. Damaged condition of ST80 beam after the test

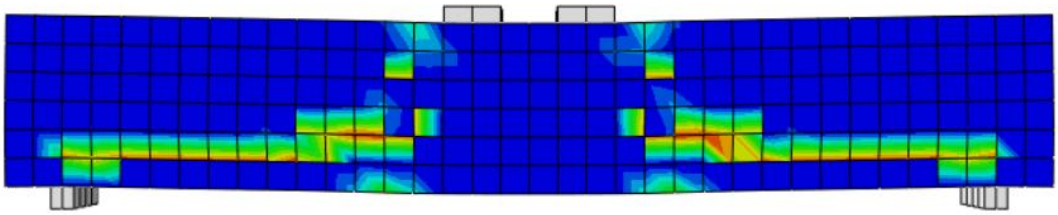

Figure 4.7. ST80 beam numerical analysis result

The condition of the reinforced concrete beam specimens modelled in ABAQUS programme after being subjected to the same loading as the experiment is shown in Figure 4.7.

The results of the parametric study for the ST80 beam with a yield strength fy = 220 MPa are given in Figure 4.8. In the graph, it is seen that as the stirrup thickness increases, the midpoint maximum displacement value and the maximum shear loads taken by the specimens before failure increase. The midpoint displacement value of the ST80_50_220 model is 6.91 mm. The maximum shear load of the specimen at this displacement value is 123.49 kN. The midpoint displacement value of the ST80_100_220 model is 7.71 mm. The maximum shear load of the specimen at this displacement value is 133.17 kN.

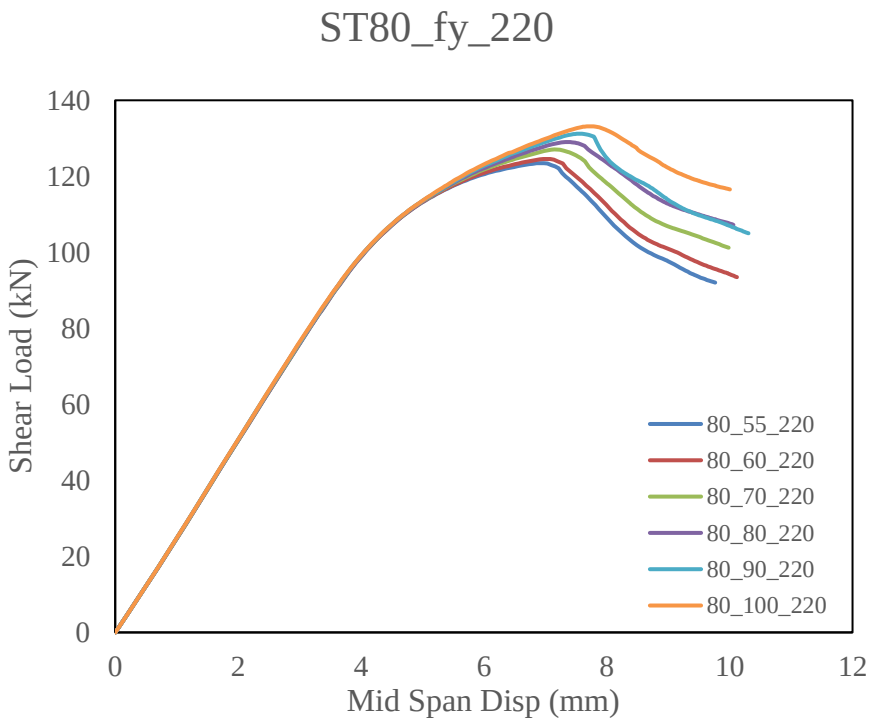

Figure 4.8. Numerical analysis behavior graphs of ST80_fy_220 specimen

The results of the parametric study for ST80 beam with stirrup yield strength fy = 310 MPa are given in Figure 4.9. In the graph, it is seen that as the stirrup thickness increases, the midpoint maximum displacement value and the maximum shear loads taken by the specimens before failure increase. The midpoint displacement value of the ST80_55_310 model is 7.09 mm. The maximum shear load of the specimen at this displacement value is 124.68 kN. The midpoint displacement value of ST80_100_310 model is 7.95 mm. The maximum shear load of the specimen at this displacement value is 135.39 kN.

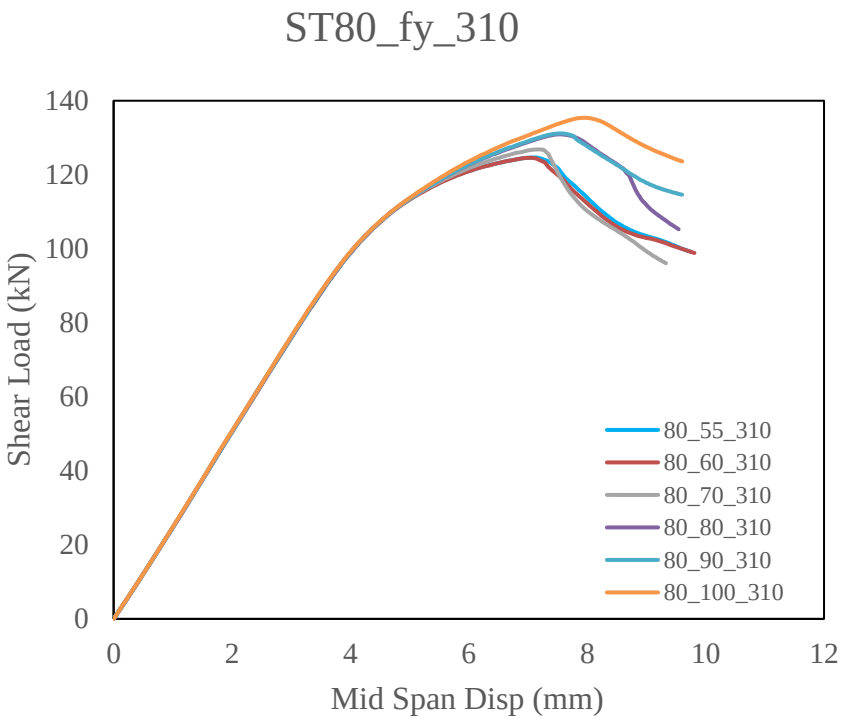

Figure 4.9. Numerical analysis behavior graphs of ST80_fy_310 specimen

The results of the parametric study for ST80 beam with stirrup yield strength fy = 420 MPa are given in Figure 4.10. In the graph, it is seen that as the stirrup thickness increases, the midpoint maximum displacement value and the maximum shear loads taken by the specimens before failure increase. The midpoint displacement value of the ST80_55_420 model is 6.91 mm. The maximum shear load of the specimen at this displacement value was 123.48 kN. The midpoint displacement value of the ST80_100_420 model is 7.73 mm. The maximum shear load of the specimen at this displacement value is 131.72 kN

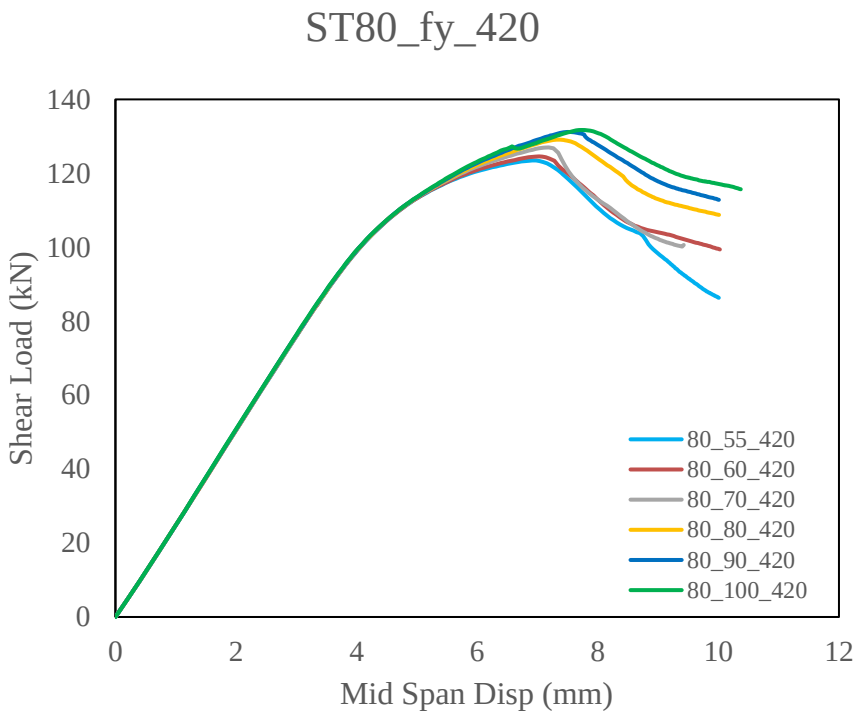

Figure 4.10. Numerical analysis behavior graphs of ST80_fy_420 specimen

The results of the parametric study for ST120 beam with stirrup yield strength fy = 220 MPa are given in Figure 4.11. In the graph, it is seen that as the stirrup thickness increases, the midpoint maximum displacement value and the maximum shear loads taken by the specimens before failure increase. The midpoint displacement value of the ST120_55_220 model is 7.43 mm. The maximum shear load of the specimen at this displacement value was 108.62 kN. The midpoint displacement value of the ST120_100_220 model is 7.05 mm. The maximum shear load of the specimen at this displacement value is 115.97 kN.

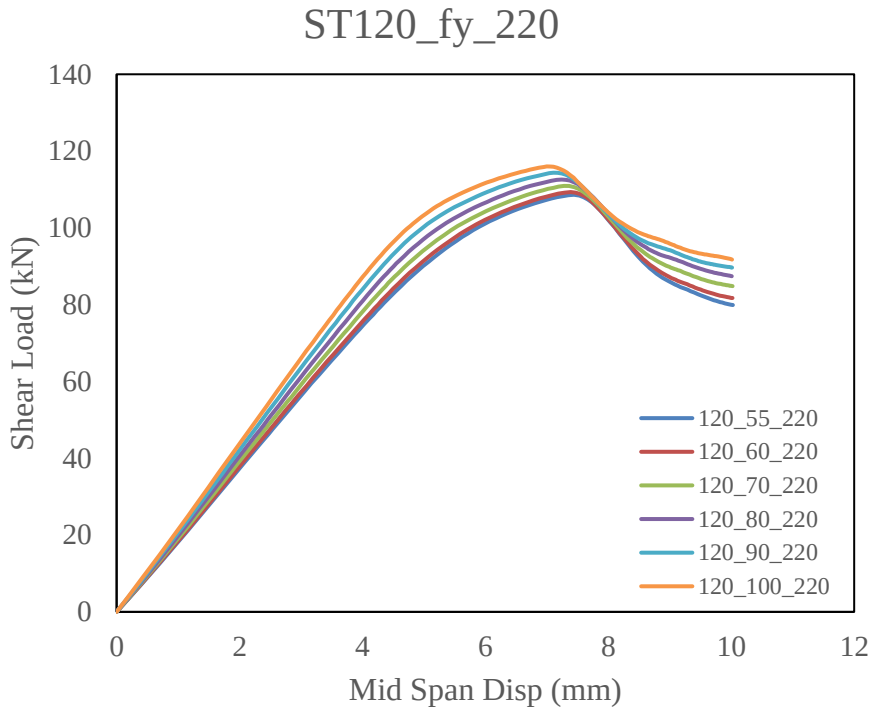

Figure 4.11. Numerical analysis behavior graphs of ST120_fy_220 specimen

The results of the parametric study for ST120 beam with stirrup yield strength fy = 310 MPa are given in Figure 4.12. In the graph, it is seen that as the stirrup thickness increases, the midpoint maximum displacement value and the maximum shear loads taken by the specimens before failure increase. The midpoint displacement value of the ST120_55_310 model is 7.43 mm. The maximum shear load of the specimen at this displacement value is 108.54 kN. The midpoint displacement value of the ST120_100_310 model is 7.05 mm. The maximum shear load of the specimen at this displacement value is 115.97 kN.

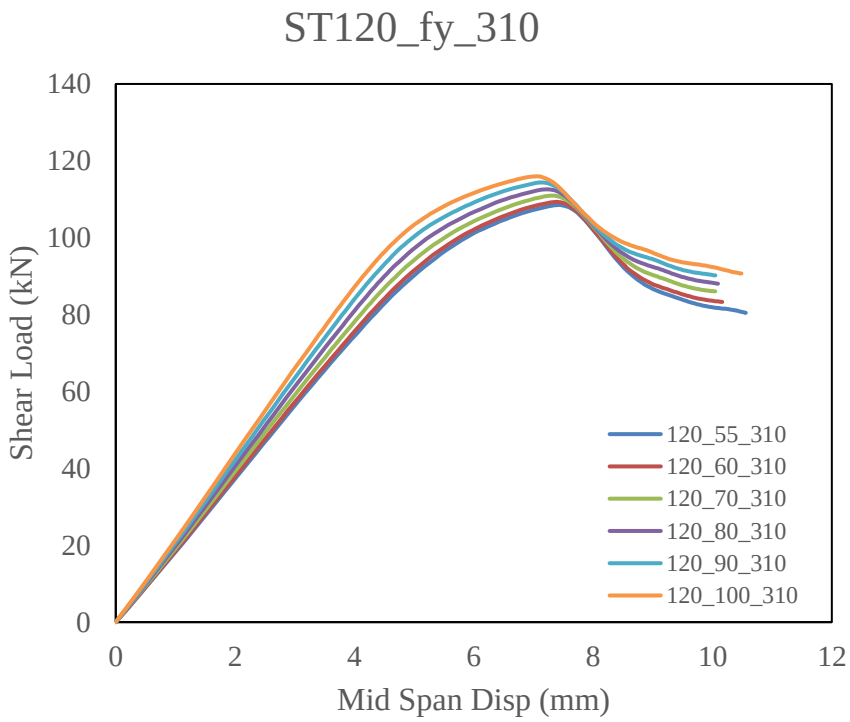

Figure 4.12. Numerical analysis behavior graphs of ST120_fy_310 specimen

The results of the parametric study for ST120 beam with stirrup yield strength fy = 420 MPa are given in Figure 4.13. In the graph, it is seen that as the stirrup thickness increases, the midpoint maximum displacement value and the maximum shear loads taken by the specimens before failure increase. The midpoint displacement value of the ST120_55_420 model is 7.43 mm. The maximum shear load of the specimen at this displacement value is 108.54 kN. The midpoint displacement value of the ST120_100_420 model is 7.05 mm. The maximum shear load of the specimen at this displacement value is 115.97 kN.

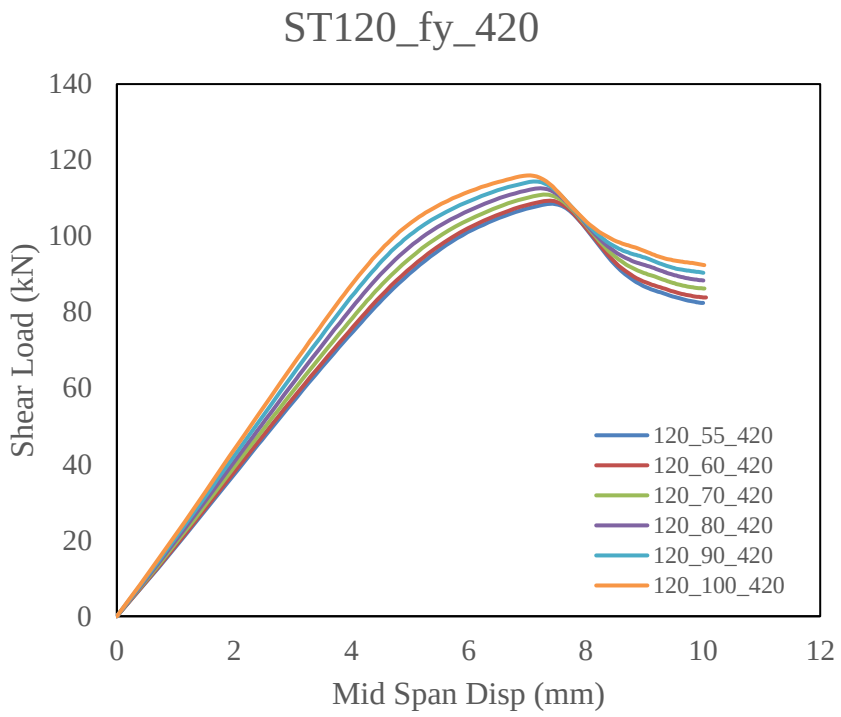

Figure 4.13. Numerical analysis behavior graphs of ST120_fy_420 specimen

In table 4.1 and table 4.2, the results of the parametric study modelled in ABAQUS programme are compared with the results of the experiment and the calculations made with the formulas in ACI 318-02, Eurocode 2 and TS500 regulations.

Table 4.1. ST80 Comparison of experimental and parametric results with design code calculations

	Experiment	ABAQUS	ACI 318-02	EuroCode2	TS500
80_5.5_220		123.49	83.08	62.06	67.21
80_5.5_310	125.22	124.68	97.51	87.45	81.1
80_5.5_420		123.48	115.15	118.48	98.08
80_6_220		124.58	89.78	73.86	73.67
80_6_310		124.57	106.96	104.06	90.2
80_6_420		124.58	127.96	141	110
80_7_220		127.03	104.94	100.53	88.26
80_7_310		126.87	128.32	141.65	110.76
80_7_420		127.01	156.9	191.92	138.26
80_8_220		129	122.44	131.3	105.1
80_8_310		130.94	152.98	185.04	134.49
80_8_420		129.1	190.3	250.06	170.41
80_9_220		131.197	142.27	166.18	124.18
80_9_310		131.17	180.91	234.17	161.38
80_9_420		131.177	228.15	317.26	206.84
80_10_220		133.175	164.43	205.16	145.51

Table 4.2. (Continued) ST80 Comparison of experimental and parametric results with design code calculations

80_10_310	135.39	212.14	289.1	191.43
80_10_420	131.72	270.46	391.68	247.56

Table 4.2. ST120 Comparison of experimental and parametric results with design code calculations

	Experiment	**ABAQUS**	**ACI 318-02**	**EuroCode2**	**TS500**
120_5.5_220		108.623	71.32	41.37	55.89
120_5.5_310	107.03	108.54	80.94	58.30	65.15
120_5.5_420		108.54	92.7	78.99	76.47
120_6_220		109.323	75.79	49.24	60.2
120_6_310		109.33	87.24	69.37	71.22
120_6_420		109.33	101.23	94.00	84.69
120_7_220		110.931	85.89	67.02	69.92
120_7_310		110.943	101.48	94.43	84.93
120_7_420		110.943	120.53	127.95	103.26
120_8_220		112.585	97.56	87.53	81.15
120_8_310		112.596	117.92	123.36	100.74
120_8_420		112.596	142.8	166.71	124.69
120_9_220		114.365	110.78	110.79	93.87
120_9_310		114.373	136.54	156.11	118.67
120_9_420		114.373	168.03	211.51	148.98
120_10_220		115.977	125.55	136.77	108.09
120_10_310		115.978	157.36	192.73	138.71
120_10_420		115.978	196.24	261.12	176.12

5. CONCLUSION AND FUTURE WORKS

The aim of this thesis is to investigate the parameters affecting the shear capacity of reinforced concrete beams by numerical modelling methods. For this purpose, the parameters affecting the shear capacity of reinforced concrete beams were investigated in a 4-stage study. In the first stage, 2 experiments with shear failure damage available in the literature were selected. In the second stage, these experiments were modelled in ABAQUS programme using finite element method. Experimental results and numerical modelling results were compared. The results were found to be similar and the accuracy of the model was accepted. In the third stage, geometry, material properties and size were kept constant. Parametric study was performed by changing the stirrup thickness. Then, a study was carried out according to the yield strength of S220 and S420 steel and the study was extended. A total of 36 reinforced concrete beams were modelled. Of these models, 18 were modelled for 80 mm stirrup spacing and 18 were modelled for 120 mm stirrup spacing. In the fourth and final stage, the results of the parametric study modelled in ABAQUS programme were compared with the experimental results and calculations made with the formulas in ACI 318-02, Eurocode 2 and TS500 regulations.

The results are summarised as follows:.

- It is seen that shear failure in reinforced concrete beams can be modelled successfully by finite element method. However, parametric studies show that as the stirrup thickness in the numerical models is increased, the shear force that the reinforced concrete beams can withstand does not increase as much as it increases in the regulations.
- In parametric studies with S220 and S420 steels, no difference in the behaviour compared to S310 steel has been found.
- Numerical modelling of shear failure of reinforced concrete beams, beam-truss difference is presented. Beam models were found to reflect the shear failure behaviour much better than truss models.

- Numerical modelling was used to validate the experiment and to see how much the mesh sensitivity calibration changes the results. The accuracy of numerical modelling without mesh sensitivity should be doubted.

REFERENCES

Adebar, P., & van Leeuwen, J. (1999). Side-face reinforcement for flexural and diagonal cracking in large concrete beams. *Structural Journal*, *96*(5), 693–705.

De Silva, S., Mutsuyoshi, H., Witchukreangkrai, E., & Uramatsu, T. (2005). Analysis of shear cracking behavior in partially prestressed concrete beams. *Proceedings of JCI*, *27*(2), 865–870.

Demir, A. (2018). *Betonarme yüksek kirişlerde kesme çatlağının artık yük taşıma kapasitesine etkisinin incelenmesi* [PhD Thesis].

Demir, A., Caglar, N., Ozturk, H., & Sumer, Y. (2016). Nonlinear finite element study on the improvement of shear capacity in reinforced concrete T-Section beams by an alternative diagonal shear reinforcement. *Engineering Structures*, *120*, 158–165.

Demirtaş, G. (2019). *Çarpma Etkisindeki Ultra Yüksek Performanslı Lifli Betonarme Kirişlerin Sonlu Elemanlar Analizi*. Sakarya Üniversitesi.

Demirtaş, G., Çağlar, N., & Sümer, Y. (2018). Çarpma Etkisindeki UltraYüksek Performanslı Lifli Betonarme Kirişlerin Sonlu Elemanlar Analizi. *Academic Perspective Procedia*, *1*(1), 1126–1135.

Doğangün, A. (2019). *Betonarme yapıların hesap ve tasarımı*. Birsen yayınevi.

Earij, A., Alfano, G., Cashell, K., & Zhou, X. (2017). Nonlinear three–dimensional finite–element modelling of reinforced–concrete beams: Computational challenges and experimental validation. *Engineering Failure Analysis*, *82*, 92–115.

Ersoy, U., Ozcebe, G., & Tankut, T. (2012). *Reinforced Concrete*. Metu Press.

Hibbitt, H., Karlsson, B., & Sorensen, E. (2013). *ABAQUS 2018 Research Edition*. ABAQUS Unified FEA.

Hibbitt, K., & Karlsson, B. (2013). Sorensen: ABAQUS: User's Manual. *Hibbitt, Karlsson & Sorensen*.

Karayannis, C. G., & Chalioris, C. E. (2013). Shear tests of reinforced concrete beams with continuous rectangular spiral reinforcement. *Construction and Building Materials*, *46*, 86–97.

Kim, W., & White, R. N. (1991). Initiation of shear cracking in reinforced concrete beams with no web reinforcement. *Structural Journal*, *88*(3), 301–314.

Lee, J., & Fenves, G. L. (1998). Plastic-damage model for cyclic loading of concrete structures. *Journal of Engineering Mechanics*, *124*(8), 892–900.

Lubliner, J., Oliver, J., Oller, S., & Onate, Ejij. (1989). A plastic-damage model for concrete. *International Journal of Solids and Structures*, *25*(3), 299–326.

Mander, J. B., Priestley, M. J. N., & Park, R. (1988). Theoretical Stress-Strain Model for Confined Concrete. *Journal of Structural Engineering*, *114*(8), 1804–1826. https://doi.org/10.1061/(ASCE)0733-9445(1988)114:8(1804)

Sato, Y., Tadokoro, T., & Ueda, T. (2004). Diagonal Tensile Failure Mechanism of Reinforced Concrete Beams. *Journal of Advanced Concrete Technology*, *2*(3), 327–341. https://doi.org/10.3151/jact.2.327

Słowik, M. (2014). Shear Failure Mechanism in Concrete Beams. *Procedia Materials Science*, *3*, 1977–1982. https://doi.org/10.1016/j.mspro.2014.06.318

Sümer, Y. (2010). *FRP elemanlarla güçlendirilmiş hasarlı betonarme kirişlerin doğrusal olmayan sonlu elemanlar yöntemiyle analizi* [PhD Thesis]. Sakarya Üniversitesi.

Tatar, T., Pimentel, M., Castro, J., & Marques, M. (2017). Numerical modelling and calibration of RC columns under axial load. *COMPDYN 2017-Proceedings of the 6th International Conference on Computational Methods in Structural Dynamics and Earthquake Engineering*.

TS500. (2000). Türk Standardları Enstitüsü.

Türkiye Bina Deprem Yönetmeliği. (2018). Afet ve Acil Durum Yönetimi Başkanlığı.

Ueda, T., Pantaratorn, N., & Sato, Y. (1995). *Finite Element Analysis on Shear Resisting Mechanism of Concrete Beams with Shear Reinforcement*.

Witchukreangkrai, E. (2004). Control of diagonal cracking in partially prestressed concrete beams. *コンクリート工学年次論文集= Proceedings of the Japan Concrete Institute/日本コンクリート工学協会 編*, *26*(2), 727–732.

Witchukreangkrai, E., Mutsuyoshi, H., Takagi, M., & De Silva, S. (2006). Evaluation of shear crack width in partially prestressed concrete members. *Proceedings of JCI*, *28*(2), 823–828.

Zakaria, M., Ueda, T., Wu, Z., & Meng, L. (2009). Experimental Investigation on Shear Cracking Behavior in Reinforced Concrete Beams with Shear Reinforcement. *Journal of Advanced Concrete Technology*, *7*(1), 79–96. https://doi.org/10.3151/jact.7.79

Zararis, P. D. (2003). Shear strength and minimum shear reinforcement of reinforced concrete slender beams. *Structural Journal*, *100*(2), 203–214.

CURRICULUM VITAE

Name Surname : Fazıl Abdulkadir ÇAĞLAR

EDUCATION:

- **Undergraduate** : 2019,Erciyes University,Engineering Faculty, Civil Engineer Department

PROFESSIONAL EXPERIENCE AND AWARDS

- He has been working as a research assistant at Bolu Abant İzzet Baysal University since January 2021.

PUBLICATIONS, PRESENTATIONS AND PATENTS ON THE THESIS:

- F. A. ÇAĞLAR and T. TATAR, "Calibration of RC Columns Using Fiber Elements," presented at the 5th International Symposium on Natural Hazards and Disaster Management (ISHAD2021), Sakarya, 2021.
- F. A. ÇAĞLAR and T. TATAR, "Fiber Based Modeling Strategies of RC Columns," Academic Platform Journal of Natural Hazards and Disaster Management, vol. 2, no. 2, pp. 85–95, Dec. 2021